



HAL
open science

Microparticles harbouring Sonic hedgehog morphogen improve the vasculogenesis capacity of endothelial progenitor cells derived from myocardial infarction patients

Carlos Bueno-Betí, Susana Novella, Raffaella Soleti, Ana Mompeón, Luisa Vergori, Juan Sanchís, Ramarosan Andriantsitohaina, Maria Carmen Martinez, Carlos Hermenegildo

► **To cite this version:**

Carlos Bueno-Betí, Susana Novella, Raffaella Soleti, Ana Mompeón, Luisa Vergori, et al.. Microparticles harbouring Sonic hedgehog morphogen improve the vasculogenesis capacity of endothelial progenitor cells derived from myocardial infarction patients. *Cardiovascular Research*, 2019, 115 (2), pp.409-418. 10.1093/cvr/cvy189 . hal-03048091

HAL Id: hal-03048091

<https://hal.science/hal-03048091>

Submitted on 17 Dec 2020

HAL is a multi-disciplinary open access archive for the deposit and dissemination of scientific research documents, whether they are published or not. The documents may come from teaching and research institutions in France or abroad, or from public or private research centers.

L'archive ouverte pluridisciplinaire **HAL**, est destinée au dépôt et à la diffusion de documents scientifiques de niveau recherche, publiés ou non, émanant des établissements d'enseignement et de recherche français ou étrangers, des laboratoires publics ou privés.

MICROPARTICLES HARBORING SONIC HEDGEHOG MORPHOGEN IMPROVE THE VASCULOGENESIS CAPACITY OF ENDOTHELIAL PROGENITOR CELLS DERIVED FROM MYOCARDIAL INFARCTION PATIENTS

Authors: Carlos Bueno-Betí (1,2), Susana Novella (1,2), Raffaella Soleti (3), Ana Mompeón (1,2), Luisa Vergori (3), Juan Sanchís (2,4), Ramarason Andriantsitohaina (3), María Carmen Martínez (3), and Carlos Hermenegildo (1,2).

Affiliations:

(1) Department of Physiology, Faculty of Medicine and Dentistry. University of Valencia

(2) INCLIVA Biomedical Research Institute, Valencia, Spain

(3) INSERM UMR1063, Stress oxydant et pathologies métaboliques, Université d'Angers, Angers, France

(4) Cardiology Department, Hospital Clínico Universitario and Department of Medicine, Faculty of Medicine and Dentistry. University of Valencia

Short title: Shh+ microparticles improve human EPC function

Corresponding author:

Carlos Hermenegildo MD PhD

Physiology Department, University of Valencia.

Avda. Blasco Ibáñez 15. 46010 Valencia, Spain

Tel: +34 96 3864900

e-mail: carlos.hermenegildo@uv.es

Word count: 6431

ABSTRACT

Aims: Endothelial progenitor cells (EPC) play a role in endothelium integrity maintenance and regeneration. Decreased numbers of EPC or their impaired function correlates with an increase in cardiovascular events. Thus, EPC are important predictors of cardiovascular mortality and morbidity. Microparticles carrying the morphogen Sonic hedgehog Shh (MP^{Shh+}) trigger pro-angiogenic responses, both in endothelial cells and in ischemic rodent models. Here we propose that MP^{Shh+} regulates EPC function, thus enhancing vasculogenesis, and correcting the defects in dysfunctional EPC obtained from acute myocardial infarction (AMI) patients.

Methods and Results: The mechanisms underlying Shh pathway function and nitric oxide (NO) production in EPC were evaluated. MP^{Shh+} increased both the in vitro and in vivo vasculogenic capacity of EPC isolated from adult human peripheral blood samples. MP^{Shh+} treatment significantly increased the expression of Shh signaling pathway genes (*PTCH1*, *SMO*, and *GLI1*) and masters of pro-angiogenic genes (*NOS3*, *VEGFA*, *KDR*, and *KLF2*) in EPC. Moreover, MP^{Shh+} increased both the protein expression and activity of eNOS, resulting in increased NO production. Most importantly, MP^{Shh+} improved the vasculogenesis capacity of EPC from AMI patients to levels similar to that of EPC from healthy patients. All these effects were due to the activation of Shh pathway.

Conclusions: MP^{Shh+} increases both the vasculogenesis of EPC and their capacity to produce NO, including in EPC from patients who have recently suffered an AMI. This study underscores MP^{Shh+} and EPC as potential therapeutic tools for improving vascular regeneration as a treatment for cardiovascular ischemic disease.

INTRODUCTION

Several cardiovascular risk factors can cause endothelial injury and the loss of endothelium integrity leading to endothelial dysfunction and premature development of atherosclerotic lesions¹. Endothelial progenitor cells (EPC) are actively involved in the maintenance and regeneration of endothelial integrity, both in health and in ischemic pathologies such as acute myocardial infarction (AMI) and stroke^{2,3}. EPC are mobilized from the bone marrow and are recruited by damaged endothelium to reestablish endothelium integrity⁴. Nevertheless, accumulating evidence seems to indicate that fewer EPC may be available, or that their function might be impaired, in the presence of cardiovascular diseases⁵ or cardiovascular risk factors⁶⁻⁸. Thus, it is likely that in these disease states EPC cannot properly restore endothelium integrity, subsequently increasing the likelihood of suffering cardiovascular events⁹. Therefore, the development of new therapeutic tools for improving EPC biology in the cardiovascular pathological setting is imperative.

Microparticles (MP) are small vesicles measuring 0.1 to 1 μm in diameter and with a heterogeneous composition that are shed from the plasma membrane of activated and/or apoptotic cells. In the cardiovascular system, MP are mainly produced by endothelial cells, platelets, leukocytes, erythrocytes, and smooth muscle cells¹⁰. MP may represent a novel method for promoting intercellular communication -as vectors for transporting and delivering biological messages- that could actively participate in the pathophysiology of organisms, most notably, in cardiovascular diseases^{11,12}. Moreover, because they can deliver secretory molecules such as cytokines, chemokines, growth factors, and exogenous nucleic acids, they may be useful as therapeutic tools for the treatment of different diseases¹³.

Hedgehog (Hh) signaling proteins play an essential role in regulating the morphogenesis of different tissues and organs during development in species from a wide range of phyla¹⁴. In addition to its role in development, Sonic hedgehog morphogen (Shh) has been shown to participate in cell differentiation, angiogenesis, and proliferation in human adults^{15,16}. Shh signal transduction is complex and involves three main proteins to activate the different signaling molecules required to regulate cell proliferation, apoptosis, cytoskeleton organization, angiogenesis, gene transcription and metabolism:

Patched 1 (PTCH1), Smoothed (SMO), and GLI1 family of transcription factors^{17,18}.

Engineered MP generated from T lymphocytes under mitogenic and apoptotic conditions carry the morphogen Shh (MP^{Shh+})¹⁹ and these have previously been shown to have a beneficial effect on endothelial cells in an ischemic murine model as well as in human-origin cultured endothelial cells, by improving endothelial function and favoring angiogenesis^{20,21}. MP^{Shh+} can induce nitric oxide (NO) production and reduce the reactive oxygen species present in endothelial cells, further supporting their beneficial effect on the cardiovascular system via a phosphoinositide 3-kinase (PI3K) pathway-dependent mechanism²². However, the effect of MP^{Shh+} on adult human peripheral blood-derived EPC remains to be determined. Moreover, whether MP^{Shh+} can correct the impaired function of EPC obtained from AMI patients has not yet been assessed. Thus, the aim of this present study was to test the hypothesis that MP^{Shh+} regulates EPC function, enhances vasculogenesis, and corrects the defects associated with EPC derived from AMI patients. We also evaluated the mechanisms which underlie Shh pathway and NO production in endothelial cells.

MATERIAL AND METHODS

Detailed experimental protocols are available in the Supplementary material available online.

This work conforms to the principles outlined in the Declaration of Helsinki, was approved by the INCLIVA Clinical Research Ethics Committee, and written informed consent was obtained from all the donors. The animal studies were carried out using protocols approved by the Institutional Ethics Committee at the University of Valencia and conformed to the National Institutes of Health Guide for the Care and Use of Laboratory Animals.

Endothelial progenitor cell isolation, culture, and characterization

EPC were isolated and cultured as previously described in detail by our group²³. Briefly, peripheral blood was drawn from patients diagnosed with AMI (n = 11) and healthy controls (n = 20). Mononuclear cells were then isolated by density gradient centrifugation and cultured in complete EGM-2 culture medium supplemented with 20% fetal bovine serum. After 24 hours, non-adherent cells were removed and the remaining isolated EPC were maintained at 37°C with 5% of CO₂. The endothelial nature of the cultures was confirmed by testing their ability to uptake acetylated low density lipoprotein (acLDL), bind Ulex lectin, and their expression of Von Willebrand factor (vWF).

Microparticle preparation

MP were generated from human lymphoid CEM T cell line, as previously described^{20,22}. To produce MP^{Shh+}, the cells were treated with phytohaemagglutinin for 72 hours followed by phorbol-12-myristate-13 and actinomycin D for 24 hours; MP not harboring Shh morphogen (MP^{Shh-}) were produced from CEM T cells treated only with actinomycin D for 24 hours. After treatment, the culture supernatant containing the MP was recovered, centrifuged and pelleted in sterile NaCl (0.9% w/v). Finally, MP were recovered sterile NaCl (0.9% w/v), adjusting their dilution to 10 µg MP proteins per mL (both for MP^{Shh+} and MP^{Shh-}) as the optimal concentration for angiogenesis induction^{20,21}.

Formation of capillary-like structures *in vitro*

EPC isolated from peripheral blood samples were seeded at 1.5×10^5 cells/well on 24-well plates coated with Matrigel[®] and were incubated for 24 hours, either in the presence or the absence of MP^{Shh+} (10 µg/mL) or MP^{Shh-} (10 µg/mL). In

some experiments, the SMO inhibitor cyclopamine (15 μ M) or PI3K inhibitor LY 294002 (10 μ M) were added 30 minutes before starting the treatment with MP. The desired concentrations of cyclopamine and LY294002 were obtained by successive dilutions of a stock solution with DMSO. In all the experiments, control cells were exposed to 1% DMSO to discard any effect of the vehicle. Capillary-like structure formation was recorded with a Nikon digital sight Ds-QiMc camera and Nikon Eclipse-Ti inverted microscope with a 4 \times objective (total magnification 40 \times). For each experimental condition, five random fields were selected and analyzed with Image Pro-Plus Software V.6. All measurements were conducted by an observer blinded to the experimental-group assignment.

***In vivo* Matrigel plug assay**

For *in vivo* studies of MP-induced EPC vasculogenesis, EPC were incubated in the absence or presence of MP^{Shh+} (10 μ g/mL) for 24 hours *in vitro*. Matrigel reagent was supplemented with growth factors contained in EGM-2 single quots. Matrigel plugs were prepared on ice by mixing 300 μ L of Matrigel with 7.5×10^5 EPC which had or had not been pretreated with MP^{Shh+}. These plugs were then subcutaneously injected into each hind flank of nude RjOrl:NMRI-Foxn1nu/Foxn1nu mice under isoflurane anesthesia (n=6 controls, n=6 MP^{Shh+}, n=3 cyclopamine and n=6 cyclopamine + MP^{Shh+}). Animal health was monitored daily by specialized staff; after 7 days the mice were euthanized under isoflurane anesthesia and the plugs were removed and homogenized in lysis buffer overnight at 4°C. The total hemoglobin content per plug, referred to its weight, was determined using Drabkin reagent.

Immunohistochemistry of Matrigel plugs

Frozen Matrigel plug sections (20 μ m) were incubated with primary mouse anti-human CD31 antibody and, following washing steps with PBS, with rabbit anti-human CD34. Following washes with PBS, either Alexa Fluor 488 goat anti-mouse or goat anti-rabbit Alexa Fluor 546, secondary antibodies were applied to detect CD31 and CD34, respectively. Nuclei were counterstained with 4,6-diamidino-2-phenylindole (DAPI). Confocal microscopy and digital image recording were used to calculate the vessel area using ImageJ software (National Institute of Health, USA).

Quantitative polymerase chain reaction analysis

To determine the expression of Shh pathway signaling genes as well as genes of cardiovascular interest in EPC, treated cells were recovered in TRIzol[®] reagent and total RNA isolation was performed using a PureLink[®] RNA Mini Kit. For the reverse-transcription reactions, 300 ng of total RNA was reverse transcribed using a High-Capacity cDNA reverse-transcription kit. The mRNA levels were determined by quantitative real-time PCR analysis using an ABI Prism 7900 HT Fast Real-Time PCR System (Applied Biosystems) and gene-specific primer pairs and probes with a TaqMan Universal PCR Master Mix. Each sample was analyzed in triplicate and the expression values were calculated according to the $2^{-\Delta\Delta C_t}$ method.

Determination of nitric oxide production

NO production in cultured EPC was determined using a 4-amino-5-methylamino-2',7'-difluorofluorescein (DAF-FM diacetate) fluorescent probe. First, cells were incubated for 24 hours, either in the presence or in the absence of MP^{Shh+} (10 µg/mL) or MP^{Shh-} (10 µg/mL) preincubated with or without cyclopamine (15 µM), LY 294002 (10 µM), or the NO synthase inhibitor N ω -Nitro-L-arginine methyl ester hydrochloride (L-NAME; 100 µM). After treatment, DAF-FM diacetate (3.8 µM) was added to the culture media for 30 minutes. NO production was determined by measuring DAF-FM fluorescence on a Nikon digital sight Ds-QiMc camera and Nikon Eclipse-Ti fluorescence inverted microscope (with a 10 \times objective; giving a total magnification of 100 \times). For each experimental condition, five random fields were analyzed with Image Pro-Plus Software V.6 and the mean intensity fluorescence per power field was recorded.

Western blot analysis

EPC cultures were incubated for 24 hours either in the presence or absence of MP^{Shh+} (10 µg/mL) or MP^{Shh-} (10 µg/mL) and preincubated with cyclopamine (15 µM) or LY 294002 (10 µM) for 30 minutes or not. The contents of the EPC culture wells were then recovered with RIPA buffer and the protein extracted according to standard protocols. Equal amounts of protein were separated and membranes were incubated overnight with adequate antibodies, using β -actin as a loading control. The Western blots were then subjected to densitometric analysis using MacBiophotonics plug-ins for ImageJ software.

Statistical analysis

Data normality was assessed using the Kolmogorov–Smirnov test. Values

shown in the text and figures represent the mean \pm the standard error of the mean (SEM). Statistical analysis was performed either by using Student t-tests for single comparisons or one-way analysis of variance (ANOVA) for multiple comparisons and the Newman–Keuls post-test. P values < 0.05 were considered significant. Statistical analysis was carried out using Prism software (version 5.04; GraphPad Software Inc., San Diego, CA, USA).

RESULTS

Endothelial progenitor cell isolation and characterization

All cell cultures used in the present investigation were cultured and isolated under to the most suitable conditions, as previously determined²³. All EPC cultures took on the familiar cobblestone-like morphology used to identify endothelial cells in culture (Supplementary Figure S1A). Similarly, cell cultures employed in these experiments were able to uptake acLDL and bind Ulex-Lectin -thus, indicating their endothelial cell-like phenotype (Supplementary Figure S1B)-, and expressed vWF, a multimeric glycoprotein constitutively expressed in endothelial cells (Supplementary Figure S1C). In addition, we performed immunophenotyping of these cells by flow cytometry (Supplementary Figure S2). Cultured EPC expressed the endothelial markers KDR, CD31, and CD146, whereas panleukocyte marker CD45 was absent, and progenitor the marker CD34 was found in 45% of cells. Collectively, these data demonstrated that the cultured EPC used in the present work were late EPC.

MP^{Shh+} promote *in vitro* capillary-like structure formation and *in vivo* EPC vasculogenesis

To test the effect of MP^{Shh+} on EPC function, first we studied its effect on *in vitro* vasculogenesis. Untreated EPC and those treated with MP^{Shh-} formed capillary-like structures on Matrigel matrices, but the overall structures were poorly organized (Figure 1A). In contrast, EPC treated with MP^{Shh+} for 24 hours produced significantly longer capillary-like structures than non-treated EPC (Figure 1B) which were more organized.

To assess whether MP^{Shh+} could also increase vasculogenesis *in vivo*, we performed Matrigel plug assays. Seven days after subcutaneous implantation, the retrieved plugs contained a blush of blood vessel proliferation in mice that received EPC pretreated with MP^{Shh+} for 24 hours (Figure 1C). Quantification of the hemoglobin content per plug showed that MP^{Shh+}-treated EPC plugs exhibited an increase in total hemoglobin content of 2.15 ± 0.34 -fold (Figure 1D) compared to the controls. In the presence of the selective hedgehog signaling inhibitor, cyclopamine, the effects of MP^{Shh+} in both macroscopic appearance and hemoglobin content were completely abolished.

Next, we stained the Matrigel plugs with anti-human CD31 antibody to analyze vessel density (green, Figure 1E). The CD31-positive staining showed a

proliferation and reorganization of EPC on Matrigel plugs. Moreover, the density of mature vascular structures in the MP^{Shh+}-treated EPC plugs was higher than in untreated EPC (Figure 1F), and this effect was prevented in the presence of cyclopamine. The staining of plug samples with CD34 was much less intense (red, Figure 1E) than CD31, thus reflecting a decreased progenitor capacity which was not modified by exposure to MP^{Shh+} and/or cyclopamine. Therefore, these results show that MP^{Shh+} were able to increase the *in vivo* vasculogenic capacity of EPC through an Shh-mediated pathway.

MP^{Shh+} induce Shh signaling pathway and endothelial gene expression on EPC

To analyze the pathways regulated by MP^{Shh+} in EPC, first we checked the constitutive expression of the main Shh signaling pathway components in EPC. We found that *PTCH1*, *SMO*, and *GLI1* were basally-expressed in EPC, but after treatment with MP^{Shh+} for 24 hours, their expression increased by 1.64 ± 0.05 , 1.46 ± 0.14 , and 2.57 ± 0.06 -fold, respectively. Shh pathway gene expression remained unchanged in EPC treated with MP^{Shh-} (Figure 2A). In terms of genes involved in angiogenesis, MP^{Shh+} treatment significantly increased *NOS3*, *VEGFA*, *KDR*, and *KLF2* expression by 2.94 ± 0.91 , 1.53 ± 0.17 , 1.54 ± 0.11 , and 1.76 ± 0.18 -fold, respectively (Figure 2B). However, the expression of these genes in MP^{Shh-}-treated EPC remained similar to that of non-treated EPC. These results suggest that the Shh signaling pathway is functional in EPC and can be activated by MP^{Shh+}, leading to increased expression of pro-angiogenic genes.

MP^{Shh+} promote *in vitro* capillary-like structure formation through Shh signaling pathway activation

To elucidate whether the Shh carried by MP^{Shh+} produced the increased capillary structure formation, EPC were incubated either with the selective hedgehog-signaling inhibitor, cyclopamine, or the PI3K inhibitor, LY 294002. Both these treatments prevented the formation of capillary-like structures (Figures 3A and 3B) and compared to MP^{Shh+} alone, cyclopamine or LY 294002 reduced the total capillary length by approximately 50%, from 1.82 ± 0.20 to 0.97 ± 0.13 and 0.83 ± 0.16 , respectively. Addition of the inhibitors without MP^{Shh+} had no effect on EPC capillary-like structure formation (Figure 3B).

These results indicate that Shh signaling pathway activation and PI3K activity produce the increased vasculogenic capacity of EPC treated with MP^{Shh+}.

MP^{Shh+} stimulate NO production through Shh signaling activation

Because *NOS3* expression was increased in our experiments, we studied the role of the Shh pathway in NO production in EPC exposed to MP. Treatment with MP^{Shh+} but not MP^{Shh-} stimulated NO production in EPC (Figure 4A-B). In addition, the use of the inhibitors cyclopamine and LY 294002 completely prevented the MP^{Shh+}-mediated increase in NO production. As expected, this effect was completely abolished by the presence of the NO synthase inhibitor, L-NAME (Figure 4C-D). Furthermore, MP^{Shh+} treatment had no effect on Akt protein expression nor Akt phosphorylation at its activator site—Ser 473 (Figure 5A). Interestingly, MP^{Shh+} also significantly increased eNOS protein expression and phosphorylation at its activator site (Ser 1177), while MP^{Shh+} treatment reduced eNOS phosphorylation at its inhibitory site (Thr 495; Figure 5B). Cyclopamine and LY 294002 completely abrogated the effects of MP^{Shh+} on the NO pathway in EPC, while in the absence of MP^{Shh+} NO production, protein expression, and Akt and eNOS phosphorylation were unaffected. These results show that MP^{Shh+} activate a SMO and PI3K inhibitor-sensitive mechanism, producing heightened NO production and increased eNOS protein expression and activity.

MP^{Shh+}-mediated capillary-like structure formation is NO-independent

To investigate the relationship between NO production and *in vitro* capillary-like structure formation, EPC were treated with MP^{Shh+} in the presence or absence of L-NAME for 24 hours. Although L-NAME abolished the MP^{Shh+}-induced increase in NO production (Figure 4C-D), it did not affect the increase in the total length of capillary-like structures produced by MP^{Shh+} (Supplementary Figure S3).

MP^{Shh+} effect on cultured EPC isolated from acute myocardial infarction patients

We also cultured EPC isolated from the peripheral blood of patients who had suffered an AMI and tested whether MP^{Shh+} produces similar effects in these cells. The demographic and main clinical data of all participants are presented in Supplemental Table 1. Our results revealed that EPC isolated from patients

that had suffered an acute AMI had a reduced vasculogenic capacity compared to those from healthy volunteers (Figure 6A-B). MP^{Shh+} significantly increased the vasculogenic capacity of healthy donors. Interestingly, MP^{Shh+} also increased the vasculogenic capacity of EPC derived from AMI patients to similar levels to those from healthy donors. In fact, the increase in vasculogenic capacity produced by MP^{Shh+} was indistinguishable between healthy donors (160%) and AMI patients (154%). The effect of MP^{Shh+} in EPC from healthy donors was completely abolished in the presence of cyclopamine. The basal EPC expression of *NOS3*, *VEGFA*, *KDR*, and *KLF2* was not modified in AMI patients (Figure 6C). When cells were exposed to MP^{Shh+} , the expression of these genes in EPC derived from AMI patients increased to the same levels as those from healthy donors. Thus, MP^{Shh+} were able to restore the vasculogenic capacity of EPC obtained from AMI patients.

DISCUSSION

Here, we demonstrate for the first time in human EPC that MP, generated from T lymphocytes under mitogenic and apoptotic conditions and carrying the morphogen Shh, induce: (1) *in vitro* and *in vivo* vasculogenesis; (2) the expression of Shh signaling pathway genes and genes involved in vasculogenesis; (3) NO production which is directly mediated both by the Shh pathway and PI3K activation; and most importantly (4) that MP^{Shh+} improves the vasculogenic capacity of human EPC isolated from AMI patients.

EPC are capable of postnatal vasculogenesis and so are a mechanism for endothelial maintenance and repair because they counteract ongoing endothelial cell injury, replace dysfunctional endothelia, and enhance tissue repair after ischemic vascular injury^{2,24,25}. Among the different EPC sources, human EPC can be isolated and expanded from peripheral blood²³ making them easily to manipulate in laboratory conditions. The cells we isolated here were likely true late EPC, because, in addition to their morphologic characterization (Supplemental figure S1), the EPC obtained using this protocol were positive for the expression of endothelial markers CD31, KDR, CD146, the progenitor marker CD34, and negative for the expression of the panleukocyte marker CD45 (Supplemental figure S2), as previously demonstrated²³.

Revascularization by autologous patient-derived EPC is a promising therapeutic strategy for enhancing vascular repair in ischemic diseases^{26,27} and represents a significantly expanding field²⁸. However, we still lack knowledge of the mechanisms that control EPC function and how this might be augmented.

The use of MP^{Shh+} is one of the most promising developments in the field of cardiovascular medicine and regenerative therapy^{13,21}. Here we demonstrate that MP^{Shh+} can improve the vasculogenic capacity of human EPC *in vitro*, by increasing both the total length and the apparent integrity of EPC-derived tube-like structures. Indeed, this effect is comparable to that previously found for MP^{Shh+} used in human endothelial cells cultured *in vitro*²⁰. The same study also showed that silencing the Shh receptor PTCH1 and pharmacological SMO inhibition with cyclopamine abrogated the effects of MP^{Shh+}, suggesting that its ability to enhance vasculogenesis might be mediated by Hh signaling pathway activation. Accordingly, in two different endothelial cell models, Shh pathway

activation by recombinant Shh induces cyclopamine-sensitive capillary morphogenesis by rapidly activating PI3K and transcriptionally-regulated pathways²⁹.

Our results also indicate that the effect of MP^{Shh+} on EPC *in vitro* is preserved *in vivo* because nude mice implanted with MP^{Shh+}-treated human EPC Matrigel plugs develop more capillaries than controls, in a Shh-dependent manner, thus reinforcing the role MP^{Shh+} plays in augmenting vasculogenesis. MP^{Shh+} was previously found to promote neovascularization *in vivo* in a mouse model of hind limb ischemia by stimulating vascular density and blood flow recovery in ischemic limbs after femoral artery ligation²¹. Thus, MP^{Shh+} also improves the vasculogenic function of human EPC isolated from peripheral blood.

In terms of gene expression, our study revealed that *PTCH1*, *SMO*, and *GLI1*, the main members of the Hh signaling pathway, are basally expressed in EPC isolated from peripheral blood samples. Moreover, treating EPC with MP^{Shh+} increases the expression of these genes suggesting activation of the canonical Hh signaling pathway. This concurs with results from Hh-treated bone marrow-derived EPC and primitive human hematopoietic cells^{30,31}. However, HUVEC³² as well as the isolated, expanded, and cultured EPC we used in this study respond differently to Shh. In this sense, it is likely that HUVEC and mature endothelial cells only activate non-canonical responses upon Shh treatment³², while EPC probably activate both canonical and non-canonical responses.

Of note, MP^{Shh+} increases the expression its receptor, SMO. This effect was first demonstrated in *Drosophila*³³ but has also been demonstrated in other experimental models, such as adult motor neurons in rat axotomy³⁴ or in cell hypoxia³⁵, suggesting that Shh may stimulate SMO in an autocrine manner.

In human EPC, MP^{Shh+} induces a cyclopamine-sensitive increase in the mRNA expression of several genes involved in vasculogenesis and NO production, including *VEGF*, *KDR*, *KLF2*, and *eNOS*. This indicates that Shh carried by MP acts on several target genes that regulate vascular function at different levels. Previous studies show that MP^{Shh+} improves endothelial function in the mouse aorta and favors *in vitro*²⁰ and *in vivo* angiogenesis²¹ by increasing NO production through eNOS activity. Surprisingly, inhibition of NO production with

L-NAME does not affect the EPC vasculogenic capacity induced by MP^{Shh+}, suggesting that this effect does not result from MP^{Shh+}-mediated NO production.

Use of the selective inhibitors cyclopamine and LY 294002, completely abrogated the increase in EPC vasculogenic capacity induced by MP^{Shh+}, suggesting that this effect is mainly mediated by mechanisms directly dependent on SMO and PI3K. Our results demonstrate that in EPC, MP^{Shh+} acts via Shh signaling pathway activation and also involves PI3K pathway participation. This mechanism of action is similar to one previously described for endothelial cells treated either with MP^{Shh+20} or with recombinant Shh protein²⁹. However, the ultimate cause of the increase in EPC vasculogenic capacity may also be related to increased VEGFA expression as there is *in vivo* evidence suggesting that the effects of Shh on wound healing are facilitated by increased VEGF-mediated neovascularization and do not result only from stimulating re-epithelialization³⁰. More recently, Renault et al. have shown that Shh-corneal angiogenesis is mediated by activation of the SMO and Rho/ROCK pathways but not by the expression of GLI transcription factors³⁶.

MP^{Shh-}, MP generated under apoptotic conditions and which do not harbor Shh morphogen, have no effect on EPC gene expression, NO production, or vasculogenesis. However, even though these MP do not contain Shh, we cannot exclude the possibility that MP^{Shh+} may contain other proteins not present in MP^{Shh-}, and that this could potentially influence or even potentiate the changes we observed in this study. In fact, MP^{Shh+} can increase the expression of different of proangiogenic factors in endothelial cells^{20,21}, and not all of these factors are regulated in a Shh-dependent manner²¹.

A recent study demonstrated blood outgrowth endothelial cells retain a robust proangiogenic profile with a therapeutic potential for targeting ischemic disease³⁷. In other studies, however, EPC isolated from patients suffering AMI presented a reduced vasculogenic capacity compared to those of EPC isolated from healthy patients. This reinforces evidence that EPC from AMI patients exhibit altered functional behavior, as measured by cell adhesion or calcium influx³⁸. Interestingly, here we demonstrate that MP^{Shh+} treatment can be used to improve the vasculogenesis of EPC derived from AMI patients to levels similar to those found in healthy volunteers, also in a Shh-dependent manner.

In that sense, other authors have recently reported that Shh-modified human CD34 cells preserved cardiac function after infarction through the exosome-mediated delivery of Shh³⁹. Therefore, activating Shh signaling through MP^{Shh+} treatment may rescue cultured EPC function and could potentially be used to promote neovascularization in AMI patients.

In conclusion, our results indicate that MP^{Shh+} exerts a positive effect on EPC by increasing their vasculogenic and NO production capacities through the Shh pathway. This effect is maintained in EPC isolated from human peripheral blood samples from patients suffering AMI and in whom both vasculogenic and NO production are impaired. Taken together our results are sufficient to propose the use of MP^{Shh+} and EPC as a potential therapeutic tool for improving vascular regeneration in patients affected by ischemic diseases such as AMI.

FUNDING

This work was supported by the Spanish Ministerio de Economía y Competitividad, Instituto de Salud Carlos III – FEDER-ERDF (grants FIS PI13/00617, FIS PI16/00229, and RD12/0042/0052) and from INSERM and University of Angers (France).

ACKNOWLEDGEMENTS

The authors thank A. Díaz (Central Research Unit of Medicine, University of Valencia) for technical assistance in the *in vivo* Matrigel plug experiments.

CONFLICT OF INTEREST

None declared

REFERENCES

1. Libby P. Fanning the flames: inflammation in cardiovascular diseases. *Cardiovasc Res.* 2015;**107**:307-309.
2. Shantsila E, Watson T, Lip GYH. Endothelial Progenitor Cells in Cardiovascular Disorders. *J Am Coll Cardiol.* 2007;**49**:741-752.
3. Tongers J, Losordo DW, Landmesser U. Stem and progenitor cell-based therapy in ischaemic heart disease: promise, uncertainties, and challenges. *Eur Heart J.* 2011;**32**:1197-1206.
4. Werner N, Junk S, Laufs U, Link A, Walenta K, Böhm M, Nickenig G. Intravenous Transfusion of Endothelial Progenitor Cells Reduces Neointima Formation After Vascular Injury. *Circ Res.* 2003;**93**:e17.
5. Dong C, Goldschmidt-Clermont PJ. Endothelial Progenitor Cells: A Promising Therapeutic Alternative for Cardiovascular Disease. *J Interven Cardiol.* 2007;**20**:93-99.
6. Krenning G, Dankers PYW, Drouven JW, Waanders F, Franssen CFM, van Luyn MJA, Harmsen MC, Popa ER. Endothelial progenitor cell dysfunction in patients with progressive chronic kidney disease. *Am J Physiol - Renal Physiol.* 2009;**296**:F1314-F1322.
7. Tepper OM, Galiano RD, Capla JM, Kalka C, Gagne PJ, Jacobowitz GR, Levine JP, Gurtner GC. Human Endothelial Progenitor Cells From Type II Diabetics Exhibit Impaired Proliferation, Adhesion, and Incorporation Into Vascular Structures. *Circulation.* 2002;**106**:2781.
8. Imanishi T, Hano T, Sawamura T, Nishio I. Oxidized low-density lipoprotein induces endothelial progenitor cell senescence, leading to cellular dysfunction. *Clin Exp Pharmacol Physiol.* 2004;**31**:407-413.
9. Werner N, Nickenig G. Influence of Cardiovascular Risk Factors on Endothelial Progenitor Cells: Limitations for Therapy? *Arterioscler Thromb Vasc Biol.* 2006;**26**:257-266.
10. György B, Szabó TG, Pásztói M, Pál Z, Misják P, Aradi B, László V, Pállinger É, Pap E, Kittel Á, Nagy G, Falus A, Buzás EI. Membrane vesicles, current state-of-the-art: emerging role of extracellular vesicles. *Cell Mol Life Sci.* 2011;**68**:2667-2688.
11. Andriantsitohaina R, Gaceb A, Vergori L, Martínez MC. Microparticles as Regulators of Cardiovascular Inflammation. *Trends Cardiovasc Med.* 2012;**22**:88-92.
12. Martinez MC, Tual-Chalot S, Leonetti D, Andriantsitohaina R. Microparticles: targets and tools in cardiovascular disease. *Trends Pharmac Sci.* 2011;**32**:659-665.
13. Fleury A, Martínez C, Le Lay S. Extracellular vesicles as therapeutic tools in cardiovascular diseases. *Front Immunol.* 2014;**5**:370.
14. Varjosalo M, Taipale J. Hedgehog signaling. *J Cell Sci.* 2007;**120**:3-6.

15. Bailey JM, Singh PK, Hollingsworth MA. Cancer metastasis facilitated by developmental pathways: Sonic hedgehog, Notch, and bone morphogenic proteins. *J Cell Biochem.* 2007;**102**:829-839.
16. Ingham PW, McMahon AP. Hedgehog signaling in animal development: paradigms and principles. *Genes Dev.* 2001;**15**:3059-3087.
17. Robbins DJ, Fei DL, Riobo NA. The Hedgehog Signal Transduction Network. *Sci Signal.* 2012;**5**:re6.
18. Teperino R, Aberger F, Esterbauer H, Riobo N, Pospisilik JA. Canonical and non-canonical Hedgehog signalling and the control of metabolism. *Semin Cell Dev Biol.* 2014;**33**:81-92.
19. Martínez MC, Larbret F, Zobairi F, Coulombe J, Debili N, Vainchenker W, Ruat M, Freyssinet J-M. Transfer of differentiation signal by membrane microvesicles harboring hedgehog morphogens. *Blood.* 2006;**108**:3012-3020.
20. Soleti R, Benameur T, Porro C, Panaro MA, Andriantsitohaina R, Martínez MC. Microparticles harboring Sonic Hedgehog promote angiogenesis through the upregulation of adhesion proteins and proangiogenic factors. *Carcinogenesis.* 2009;**30**:580-588.
21. Benameur T, Soleti R, Porro C, Andriantsitohaina R, Martínez MC. Microparticles Carrying Sonic Hedgehog Favor Neovascularization through the Activation of Nitric Oxide Pathway in Mice. *PLoS ONE.* 2010;**5**:e12688.
22. Agouni A, Mostefai HA, Porro C, Carusio N, Favre J, Richard V, Henrion D, Martinez MC, Andriantsitohaina R. Sonic hedgehog carried by microparticles corrects endothelial injury through nitric oxide release. *FASEB J.* 2007;**21**:2735-2741.
23. Bueno-Betí C, Novella S, Lázaro-Franco M, Pérez-Cremades D, Heras M, Sanchís J, Hermenegildo C. An affordable method to obtain cultured endothelial cells from peripheral blood. *J Cell Mol Med.* 2013;**17**:1475-1483.
24. Berger S, Aronson D, Lavie P, Lavie L. Endothelial Progenitor Cells in Acute Myocardial Infarction and Sleep-disordered Breathing. *Am J Respir Crit Care Med* 2013;**187**:90-98.
25. Grisar JC, Haddad F, Gomari FA, Wu JC. Endothelial progenitor cells in cardiovascular disease and chronic inflammation: from biomarker to therapeutic agent. *Biomark Med.* 2011;**5**:731-744.
26. Moubarik C, Guillet B, Youssef B, Codaccioni J-L, Piercecchi M-D, Sabatier F, Lionel P, Dou L, Foucault-Bertaud A, Velly L, Dignat-George F, Pisano P. Transplanted Late Outgrowth Endothelial Progenitor Cells as Cell Therapy Product for Stroke. *Stem Cell Rev.* 2010;**7**:208-220.
27. Schwarz TM, Leicht SF, Radic T, Rodriguez-Arabaolaza I, Hermann PC, Berger F, Saif J, Böcker W, Ellwart JW, Aicher A, Heeschen C. Vascular Incorporation of Endothelial Colony-Forming Cells Is Essential for Functional Recovery of Murine Ischemic Tissue Following Cell Therapy. *Arterioscler Thromb Vasc Biol.* 2012;**32**:e13-e21.

28. Bianconi V, Sahebkar A, Kovanen P, Bagaglia F, Ricciuti B, Calabrò P, Patti G, Pirro M. Endothelial and cardiac progenitor cells for cardiovascular repair: A controversial paradigm in cell therapy. *Pharmacol Ther.* 2018;**181**:156-168.
29. Kanda S, Mochizuki Y, Suematsu T, Miyata Y, Nomata K, Kanetake H. Sonic Hedgehog Induces Capillary Morphogenesis by Endothelial Cells through Phosphoinositide 3-Kinase. *J Biol Chem.* 2003;**278**:8244-8249.
30. Asai J, Takenaka H, Kusano KF, Ii M, Luedemann C, Curry C, Eaton E, Iwakura A, Tsutsumi Y, Hamada H, Kishimoto S, Thorne T, Kishore R, Losordo DW. Topical Sonic Hedgehog Gene Therapy Accelerates Wound Healing in Diabetes by Enhancing Endothelial Progenitor Cell-Mediated Microvascular Remodeling. *Circulation.* 2006;**113**:2413-2424.
31. Bhardwaj G, Murdoch B, Wu D, Baker DP, Williams KP, Chadwick K, Ling LE, Karanu FN, Bhatia M. Sonic hedgehog induces the proliferation of primitive human hematopoietic cells via BMP regulation. *Nat Immunol.* 2001;**2**:172-180.
32. Chinchilla P, Xiao L, Kazanietz MG, Riobo NA. Hedgehog proteins activate pro-angiogenic responses in endothelial cells through non-canonical signaling pathways. *Cell cycle.* 2010;**9**:570-579.
33. Chen Y, Struhl G. Dual Roles for Patched in Sequestering and Transducing Hedgehog. *Cell.* 1996;**87**:553-563.
34. Akazawa C, Tsuzuki H, Nakamura Y, Sasaki Y, Ohsaki K, Nakamura S, Arakawa Y, Kohsaka S. The Upregulated Expression of Sonic Hedgehog in Motor Neurons after Rat Facial Nerve Axotomy. *J Neurosci.* 2004;**24**:7923-7930.
35. Onishi H, Yamasaki A, Kawamoto M, Imaizumi A, Katano M. Hypoxia but not normoxia promotes Smoothed transcription through upregulation of RBPJ and Mastermind-like 3 in pancreatic cancer. *Cancer Lett.* 2016;**371**:143-150.
36. Renault M-A, Roncalli J, Tongers J, Thorne T, Klyachko E, Misener S, Volpert OV, Mehta S, Burg A, Luedemann C, Qin G, Kishore R, Losordo DW. Sonic hedgehog induces angiogenesis via Rho kinase-dependent signaling in endothelial cells. *J Mol Cell Cardiol.* 2010;**49**:490-498.
37. Dauwe D, Pelacho B, Wibowo A et al. Neovascularization Potential of Blood Outgrowth Endothelial Cells From Patients With Stable Ischemic Heart Failure Is Preserved. *J Am Heart Ass.* 2016;**5**.
38. Rigueiro A, Cuadrado-Godia E, Bueno-Betfí C et al. Mobilization of endothelial progenitor cells in acute cardiovascular events in the PROCELL study: Time-course after acute myocardial infarction and stroke. *J Mol Cell Cardiol.* 2015;**80**:146-155.
39. Mackie AR, Klyachko E, Thorne T, Schultz KM, Millay M, Ito A, Kamide CE, Liu T, Gupta R, Sahoo S, Misener S, Kishore R, Losordo DW. Sonic Hedgehog-Modified Human CD34+ Cells Preserve Cardiac Function After Acute Myocardial Infarction. *Circ Res.* 2012;**111**:312-321.

FIGURE LEGENDS

Figure 1. The capacity of EPC to form capillary-like structures *in vitro* and to induce vasculogenesis *in vivo*. EPC isolated from peripheral blood samples from healthy patients were incubated for 24 hours on a Matrigel matrix, either in the presence or in the absence of 10 µg/mL MP^{Shh+} or 10 µg/mL MP^{Shh-}. (A) Representative phase-contrast images of capillary-like structures. (B) Quantification of the total length of capillary structures. Data are expressed as mean ± SEM (each point is the average of five random fields, n = 6 independent experiments). In another set of experiments, EPC in culture were treated or without 10 µg/mL MP^{Shh+} for 24 hours, either in the presence or absence of 15 µM cyclopamine. After treatment, 7.5×10^5 EPC were mixed with 300 µL Matrigel reagent and injected subcutaneously into nude RjOrl:NMRI-Foxn1nu/Foxn1nu mice. (C) Representative macroscopic images of Matrigel plugs, 7 days after subcutaneous injection. (D) Total hemoglobin content per plug relative to the control values, expressed as mean ± SEM (n = 3-6 plugs). For quantitative analysis of angiogenesis and blood vessel architecture, EPC were visualized with green CD31 and red CD34 immunofluorescence. Nuclei were counterstained with DAPI (blue). (E) Representative images of vascular network formation in the Matrigel plug 7 days after implantation at 100× magnification are shown. (F) The relative quantity of CD31⁺ (closed symbols) and CD34⁺ (open symbols) EPC was estimated by calculating the area occupied by green and red fluorescence (pixels), respectively. Data are the mean values ± SEM (each point is the average of five random fields, n = 3 independent experiments). *p < 0.05, **p < 0.01, and ***p < 0.001.

Figure 2. Gene expression in EPC treated with MP. EPC were incubated either in the presence of 10 µg/mL MP^{Shh+} or 10 µg/mL MP^{Shh-} for 24 hours. After treatment, expression of *PTCH1*, *SMO*, *GLI1*, *NOS3*, *VEFG*, *KDR*, and *KLF2* was determined by real time quantitative PCR. (A) Shh signaling pathway gene expression. (B) Expression of genes of cardiovascular interest. Data are the mean ± SEM (n = 3–5 independent experiments, performed in different cell cultures). *p < 0.05, **p < 0.01, and ***p < 0.001.

Figure 3. *In vitro* EPC capillary-like structure formation and Shh signaling pathways. EPC were incubated either in the presence of 10 µg/mL MP^{Shh+} or 10 µg/mL MP^{Shh-} for 24 hours, preincubated or without 15 µM cyclopamine or 10 µM LY 294002, on a Matrigel matrix. (A) Representative phase-contrast images of capillary-like structures. (B) Quantification of the total length of capillary-like structures relative to the control values. Data are the mean ± SEM (each point is the average of five random fields, n = 4–10 independent experiments). *p < 0.05, **p < 0.01, and ***p < 0.001.

Figure 4. NO production induced by MP on EPC. To evaluate the involvement of the Shh signaling pathway in NO production, EPC were incubated in the presence or absence of 10 µg/mL MP^{Shh+} or 10 µg/mL MP^{Shh-} for 24 hours, pre-incubated or without 15 µM cyclopamine or 10 µM LY 294002. Cells were then loaded with the fluorescent probe DAF-FM diacetate to determine total NO-production (A) Representative fluorescence images of NO production by treated EPC. (B) Quantification of total NO production relative to the control values, is presented as mean ± SEM (n = 4–10 independent experiments, performed in different cell cultures). In another set of experiments, EPC were incubated for 24 hours in the presence or absence of 10 µg/mL MP^{Shh+}, pre-incubated or without 100 µM of the NO synthase inhibitor L-NAME, and NO production was tested. (C) Representative images of NO production by cultured EPC after different treatments. (D) Total NO production quantification, relative to the control values, is expressed as the mean ± SEM (n = 5 independent experiments, performed in different cell cultures). ***p < 0.001.

Figure 5. Regulation of NO production and the Shh signaling pathway. EPC were incubated in the presence or in the absence of 10 µg/mL MP^{Shh+} or 10 µg/mL MP^{Shh-} for 24 hours, pre-incubated or without 15 µM cyclopamine or 10 µM LY 294002. Representative western blot images and relative levels assessed by densitometry showing the effect of MP treatment on (A) total Akt and phosphorylation of Akt at Serine 473 (presented as the ratio of total and

phosphorylated protein) and (B) total eNOS expression and phosphorylation of eNOS at Serine 1177 and Threonine 495 (both presented as the ratio of total and phosphorylated protein). Data are the mean \pm SEM (n = 3–7 independent experiments, performed in different cell cultures). *p < 0.05, **p < 0.01, and ***p < 0.001.

Figure 6. The effect of MP on EPC isolated from acute myocardial infarction patients. EPC were isolated from peripheral blood samples from healthy donors (HD) and acute myocardial infarction patients (AMI). EPC were incubated for 24 hours either in the presence or in the absence of 10 μ g/mL MP^{Shh+}, preincubated or without 15 μ M cyclopamine, on a Matrigel matrix. (A) Representative phase-contrast images of capillary-like structures. (B) Total length quantification of capillary structures formed on the Matrigel matrices were expressed relative to healthy donor values as the mean \pm SEM (each point is the average of five random fields, n = 5–11 independent experiments). (C) After treatment, expression of genes of cardiovascular interest (*NOS3*, *VEFG*, *KDR*, and *KLF2*) was determined by real time quantitative PCR. Data are the mean \pm SEM (n = 7–8 independent experiments, performed in different cell cultures). *p < 0.05, **p < 0.01, and ***p < 0.001.

MICROPARTICLES HARBORING SONIC HEDGEHOG MORPHOGEN IMPROVE THE VASCULOGENESIS CAPACITY OF ENDOTHELIAL PROGENITOR CELLS DERIVED FROM MYOCARDIAL INFARCTION PATIENTS

Authors: Carlos Bueno-Betí (1,2), Susana Novella (1,2), Raffaella Soleti (3), Ana Mompeón (1,2), Luisa Vergori (3), Juan Sanchís (2,4), Ramaroson Andriantsitohaina (3), María Carmen Martínez (3), and Carlos Hermenegildo (1,2).

Affiliations:

- (1) Department of Physiology, Faculty of Medicine and Dentistry. University of Valencia
- (2) INCLIVA Biomedical Research Institute, Valencia, Spain
- (3) INSERM UMR1063, Stress oxydant et pathologies métaboliques, Université d'Angers, Angers, France
- (4) Cardiology Department, Hospital Clínico Universitario and Department of Medicine, Faculty of Medicine and Dentistry. University of Valencia

Short title: Shh+ microparticles improve human EPC function

Corresponding author:

Carlos Hermenegildo MD PhD
Physiology Department, University of Valencia.
Avda. Blasco Ibáñez 15. 46010 Valencia, Spain
Tel: +34 96 3864900
e-mail: carlos.hermenegildo@uv.es

Word count: 6431

ABSTRACT

Aims: Endothelial progenitor cells (EPC) play a role in endothelium integrity maintenance and regeneration. Decreased numbers of EPC or their impaired function correlates with an increase in cardiovascular events. Thus, EPC are important predictors of cardiovascular mortality and morbidity. Microparticles carrying the morphogen Sonic hedgehog Shh (MP^{Shh+}) trigger pro-angiogenic responses, both in endothelial cells and in ischemic rodent models. Here we propose that MP^{Shh+} regulates EPC function, thus enhancing vasculogenesis, and correcting the defects in dysfunctional EPC obtained from acute myocardial infarction (AMI) patients.

Methods and Results: The mechanisms underlying Shh pathway function and nitric oxide (NO) production in EPC were evaluated. MP^{Shh+} increased both the in vitro and in vivo vasculogenic capacity of EPC isolated from adult human peripheral blood samples. MP^{Shh+} treatment significantly increased the expression of Shh signaling pathway genes (*PTCH1*, *SMO*, and *GLI1*) and masters of pro-angiogenic genes (*NOS3*, *VEGFA*, *KDR*, and *KLF2*) in EPC. Moreover, MP^{Shh+} increased both the protein expression and activity of eNOS, resulting in increased NO production. Most importantly, MP^{Shh+} improved the vasculogenesis capacity of EPC from AMI patients to levels similar to that of EPC from healthy patients. All these effects were due to the activation of Shh pathway.

Conclusions: MP^{Shh+} increases both the vasculogenesis of EPC and their capacity to produce NO, including in EPC from patients who have recently suffered an AMI. This study underscores MP^{Shh+} and EPC as potential therapeutic tools for improving vascular regeneration as a treatment for cardiovascular ischemic disease.

INTRODUCTION

Several cardiovascular risk factors can cause endothelial injury and the loss of endothelium integrity leading to endothelial dysfunction and premature development of atherosclerotic lesions¹. Endothelial progenitor cells (EPC) are actively involved in the maintenance and regeneration of endothelial integrity, both in health and in ischemic pathologies such as acute myocardial infarction (AMI) and stroke^{2,3}. EPC are mobilized from the bone marrow and are recruited by damaged endothelium to reestablish endothelium integrity⁴. Nevertheless, accumulating evidence seems to indicate that fewer EPC may be available, or that their function might be impaired, in the presence of cardiovascular diseases⁵ or cardiovascular risk factors⁶⁻⁸. Thus, it is likely that in these disease states EPC cannot properly restore endothelium integrity, subsequently increasing the likelihood of suffering cardiovascular events⁹. Therefore, the development of new therapeutic tools for improving EPC biology in the cardiovascular pathological setting is imperative.

Microparticles (MP) are small vesicles measuring 0.1 to 1 μm in diameter and with a heterogeneous composition that are shed from the plasma membrane of activated and/or apoptotic cells. In the cardiovascular system, MP are mainly produced by endothelial cells, platelets, leukocytes, erythrocytes, and smooth muscle cells¹⁰. MP may represent a novel method for promoting intercellular communication -as vectors for transporting and delivering biological messages- that could actively participate in the pathophysiology of organisms, most notably, in cardiovascular diseases^{11,12}. Moreover, because they can deliver secretory molecules such as cytokines, chemokines, growth factors, and exogenous nucleic acids, they may be useful as therapeutic tools for the treatment of different diseases¹³.

Hedgehog (Hh) signaling proteins play an essential role in regulating the morphogenesis of different tissues and organs during development in species from a wide range of phyla¹⁴. In addition to its role in development, Sonic hedgehog morphogen (Shh) has been shown to participate in cell differentiation, angiogenesis, and proliferation in human adults^{15,16}. Shh signal transduction is complex and involves three main proteins to activate the different signaling molecules required to regulate cell proliferation, apoptosis, cytoskeleton organization, angiogenesis, gene transcription and metabolism:

Patched 1 (PTCH1), Smoothed (SMO), and GLI1 family of transcription factors^{17,18}.

Engineered MP generated from T lymphocytes under mitogenic and apoptotic conditions carry the morphogen Shh (MP^{Shh+})¹⁹ and these have previously been shown to have a beneficial effect on endothelial cells in an ischemic murine model as well as in human-origin cultured endothelial cells, by improving endothelial function and favoring angiogenesis^{20,21}. MP^{Shh+} can induce nitric oxide (NO) production and reduce the reactive oxygen species present in endothelial cells, further supporting their beneficial effect on the cardiovascular system via a phosphoinositide 3-kinase (PI3K) pathway-dependent mechanism²². However, the effect of MP^{Shh+} on adult human peripheral blood-derived EPC remains to be determined. Moreover, whether MP^{Shh+} can correct the impaired function of EPC obtained from AMI patients has not yet been assessed. Thus, the aim of this present study was to test the hypothesis that MP^{Shh+} regulates EPC function, enhances vasculogenesis, and corrects the defects associated with EPC derived from AMI patients. We also evaluated the mechanisms which underlie Shh pathway and NO production in endothelial cells.

MATERIAL AND METHODS

Detailed experimental protocols are available in the Supplementary material available online.

This work conforms to the principles outlined in the Declaration of Helsinki, was approved by the INCLIVA Clinical Research Ethics Committee, and written informed consent was obtained from all the donors. The animal studies were carried out using protocols approved by the Institutional Ethics Committee at the University of Valencia and conformed to the National Institutes of Health Guide for the Care and Use of Laboratory Animals.

Endothelial progenitor cell isolation, culture, and characterization

EPC were isolated and cultured as previously described in detail by our group²³. Briefly, peripheral blood was drawn from patients diagnosed with AMI (n = 11) and healthy controls (n = 20). Mononuclear cells were then isolated by density gradient centrifugation and cultured in complete EGM-2 culture medium supplemented with 20% fetal bovine serum. After 24 hours, non-adherent cells were removed and the remaining isolated EPC were maintained at 37°C with 5% of CO₂. The endothelial nature of the cultures was confirmed by testing their ability to uptake acetylated low density lipoprotein (acLDL), bind Ulex lectin, and their expression of Von Willebrand factor (vWF).

Microparticle preparation

MP were generated from human lymphoid CEM T cell line, as previously described^{20,22}. To produce MP^{Shh+}, the cells were treated with phytohaemagglutinin for 72 hours followed by phorbol-12-myristate-13 and actinomycin D for 24 hours; MP not harboring Shh morphogen (MP^{Shh-}) were produced from CEM T cells treated only with actinomycin D for 24 hours. After treatment, the culture supernatant containing the MP was recovered, centrifuged and pelleted in sterile NaCl (0.9% w/v). Finally, MP were recovered sterile NaCl (0.9% w/v), adjusting their dilution to 10 µg MP proteins per mL (both for MP^{Shh+} and MP^{Shh-}) as the optimal concentration for angiogenesis induction^{20,21}.

Formation of capillary-like structures *in vitro*

EPC isolated from peripheral blood samples were seeded at 1.5×10^5 cells/well on 24-well plates coated with Matrigel[®] and were incubated for 24 hours, either in the presence or the absence of MP^{Shh+} (10 µg/mL) or MP^{Shh-} (10 µg/mL). In

some experiments, the SMO inhibitor cyclopamine (15 μ M) or PI3K inhibitor LY 294002 (10 μ M) were added 30 minutes before starting the treatment with MP.

The desired concentrations of cyclopamine and LY294002 were obtained by successive dilutions of a stock solution with DMSO. In all the experiments, control cells were exposed to 1% DMSO to discard any effect of the vehicle. Capillary-like structure formation was recorded with a Nikon digital sight Ds-QiMc camera and Nikon Eclipse-Ti inverted microscope with a 4 \times objective (total magnification 40 \times). For each experimental condition, five random fields were selected and analyzed with Image Pro-Plus Software V.6. All measurements were conducted by an observer blinded to the experimental-group assignment.

***In vivo* Matrigel plug assay**

For *in vivo* studies of MP-induced EPC vasculogenesis, EPC were incubated in the absence or presence of MP^{Shh+} (10 μ g/mL) for 24 hours *in vitro*. Matrigel reagent was supplemented with growth factors contained in EGM-2 single quots. Matrigel plugs were prepared on ice by mixing 300 μ L of Matrigel with 7.5×10^5 EPC which had or had not been pretreated with MP^{Shh+}. These plugs were then subcutaneously injected into each hind flank of nude RjOrl:NMRI-Foxn1nu/Foxn1nu mice under isoflurane anesthesia (n=6 controls, n=6 MP^{Shh+}, n=3 cyclopamine and n=6 cyclopamine + MP^{Shh+}). Animal health was monitored daily by specialized staff; after 7 days the mice were euthanized under isoflurane anesthesia and the plugs were removed and homogenized in lysis buffer overnight at 4°C. The total hemoglobin content per plug, referred to its weight, was determined using Drabkin reagent.

Immunohistochemistry of Matrigel plugs

Frozen Matrigel plug sections (20 μ m) were incubated with primary mouse anti-human CD31 antibody and, following washing steps with PBS, with rabbit anti-human CD34. Following washes with PBS, either Alexa Fluor 488 goat anti-mouse or goat anti-rabbit Alexa Fluor 546, secondary antibodies were applied to detect CD31 and CD34, respectively. Nuclei were counterstained with 4,6-diamidino-2-phenylindole (DAPI). Confocal microscopy and digital image recording were used to calculate the vessel area using ImageJ software (National Institute of Health, USA).

Quantitative polymerase chain reaction analysis

To determine the expression of Shh pathway signaling genes as well as genes of cardiovascular interest in EPC, treated cells were recovered in TRIzol[®] reagent and total RNA isolation was performed using a PureLink[®] RNA Mini Kit. For the reverse-transcription reactions, 300 ng of total RNA was reverse transcribed using a High-Capacity cDNA reverse-transcription kit. The mRNA levels were determined by quantitative real-time PCR analysis using an ABI Prism 7900 HT Fast Real-Time PCR System (Applied Biosystems) and gene-specific primer pairs and probes with a TaqMan Universal PCR Master Mix. Each sample was analyzed in triplicate and the expression values were calculated according to the $2^{-\Delta\Delta C_t}$ method.

Determination of nitric oxide production

NO production in cultured EPC was determined using a 4-amino-5-methylamino-2',7'-difluorofluorescein (DAF-FM diacetate) fluorescent probe. First, cells were incubated for 24 hours, either in the presence or in the absence of MP^{Shh+} (10 µg/mL) or MP^{Shh-} (10 µg/mL) preincubated with or without cyclopamine (15 µM), LY 294002 (10 µM), or the NO synthase inhibitor Nω-Nitro-L-arginine methyl ester hydrochloride (L-NAME; 100 µM). After treatment, DAF-FM diacetate (3.8 µM) was added to the culture media for 30 minutes. NO production was determined by measuring DAF-FM fluorescence on a Nikon digital sight Ds-QiMc camera and Nikon Eclipse-Ti fluorescence inverted microscope (with a 10× objective; giving a total magnification of 100×). For each experimental condition, five random fields were analyzed with Image Pro-Plus Software V.6 and the mean intensity fluorescence per power field was recorded.

Western blot analysis

EPC cultures were incubated for 24 hours either in the presence or absence of MP^{Shh+} (10 µg/mL) or MP^{Shh-} (10 µg/mL) and preincubated with cyclopamine (15 µM) or LY 294002 (10 µM) for 30 minutes or not. The contents of the EPC culture wells were then recovered with RIPA buffer and the protein extracted according to standard protocols. Equal amounts of protein were separated and membranes were incubated overnight with adequate antibodies, using β-actin as a loading control. The Western blots were then subjected to densitometric analysis using MacBiophotonics plug-ins for ImageJ software.

Statistical analysis

Data normality was assessed using the Kolmogorov–Smirnov test. Values

shown in the text and figures represent the mean \pm the standard error of the mean (SEM). Statistical analysis was performed either by using Student t-tests for single comparisons or one-way analysis of variance (ANOVA) for multiple comparisons and the Newman–Keuls post-test. P values < 0.05 were considered significant. Statistical analysis was carried out using Prism software (version 5.04; GraphPad Software Inc., San Diego, CA, USA).

RESULTS

Endothelial progenitor cell isolation and characterization

All cell cultures used in the present investigation were cultured and isolated under to the most suitable conditions, as previously determined²³. All EPC cultures took on the familiar cobblestone-like morphology used to identify endothelial cells in culture (Supplementary Figure S1A). Similarly, cell cultures employed in these experiments were able to uptake acLDL and bind Ulex-Lectin -thus, indicating their endothelial cell-like phenotype (Supplementary Figure S1B)-, and expressed vWF, a multimeric glycoprotein constitutively expressed in endothelial cells (Supplementary Figure S1C). In addition, we performed immunophenotyping of these cells by flow cytometry (Supplementary Figure S2). Cultured EPC expressed the endothelial markers KDR, CD31, and CD146, whereas panleukocyte marker CD45 was absent, and progenitor the marker CD34 was found in 45% of cells. Collectively, these data demonstrated that the cultured EPC used in the present work were late EPC.

MP^{Shh+} promote *in vitro* capillary-like structure formation and *in vivo* EPC vasculogenesis

To test the effect of MP^{Shh+} on EPC function, first we studied its effect on *in vitro* vasculogenesis. Untreated EPC and those treated with MP^{Shh-} formed capillary-like structures on Matrigel matrices, but the overall structures were poorly organized (Figure 1A). In contrast, EPC treated with MP^{Shh+} for 24 hours produced significantly longer capillary-like structures than non-treated EPC (Figure 1B) which were more organized.

To assess whether MP^{Shh+} could also increase vasculogenesis *in vivo*, we performed Matrigel plug assays. Seven days after subcutaneous implantation, the retrieved plugs contained a blush of blood vessel proliferation in mice that received EPC pretreated with MP^{Shh+} for 24 hours (Figure 1C). Quantification of the hemoglobin content per plug showed that MP^{Shh+}-treated EPC plugs exhibited an increase in total hemoglobin content of 2.15 ± 0.34 -fold (Figure 1D) compared to the controls. In the presence of the selective hedgehog signaling inhibitor, cyclopamine, the effects of MP^{Shh+} in both macroscopic appearance and hemoglobin content were completely abolished.

Next, we stained the Matrigel plugs with anti-human CD31 antibody to analyze vessel density (green, Figure 1E). The CD31-positive staining showed a

proliferation and reorganization of EPC on Matrigel plugs. Moreover, the density of mature vascular structures in the MP^{Shh+}-treated EPC plugs was higher than in untreated EPC (Figure 1F), and this effect was prevented in the presence of cyclopamine. The staining of plug samples with CD34 was much less intense (red, Figure 1E) than CD31, thus reflecting a decreased progenitor capacity which was not modified by exposure to MP^{Shh+} and/or cyclopamine. Therefore, these results show that MP^{Shh+} were able to increase the *in vivo* vasculogenic capacity of EPC through an Shh-mediated pathway.

MP^{Shh+} induce Shh signaling pathway and endothelial gene expression on EPC

To analyze the pathways regulated by MP^{Shh+} in EPC, first we checked the constitutive expression of the main Shh signaling pathway components in EPC. We found that *PTCH1*, *SMO*, and *GLI1* were basally-expressed in EPC, but after treatment with MP^{Shh+} for 24 hours, their expression increased by 1.64 ± 0.05 , 1.46 ± 0.14 , and 2.57 ± 0.06 -fold, respectively. Shh pathway gene expression remained unchanged in EPC treated with MP^{Shh-} (Figure 2A). In terms of genes involved in angiogenesis, MP^{Shh+} treatment significantly increased *NOS3*, *VEGFA*, *KDR*, and *KLF2* expression by 2.94 ± 0.91 , 1.53 ± 0.17 , 1.54 ± 0.11 , and 1.76 ± 0.18 -fold, respectively (Figure 2B). However, the expression of these genes in MP^{Shh-}-treated EPC remained similar to that of non-treated EPC. These results suggest that the Shh signaling pathway is functional in EPC and can be activated by MP^{Shh+}, leading to increased expression of pro-angiogenic genes.

MP^{Shh+} promote *in vitro* capillary-like structure formation through Shh signaling pathway activation

To elucidate whether the Shh carried by MP^{Shh+} produced the increased capillary structure formation, EPC were incubated either with the selective hedgehog-signaling inhibitor, cyclopamine, or the PI3K inhibitor, LY 294002. Both these treatments prevented the formation of capillary-like structures (Figures 3A and 3B) and compared to MP^{Shh+} alone, cyclopamine or LY 294002 reduced the total capillary length by approximately 50%, from 1.82 ± 0.20 to 0.97 ± 0.13 and 0.83 ± 0.16 , respectively. Addition of the inhibitors without MP^{Shh+} had no effect on EPC capillary-like structure formation (Figure 3B).

These results indicate that Shh signaling pathway activation and PI3K activity produce the increased vasculogenic capacity of EPC treated with MP^{Shh+}.

MP^{Shh+} stimulate NO production through Shh signaling activation

Because NOS3 expression was increased in our experiments, we studied the role of the Shh pathway in NO production in EPC exposed to MP. Treatment with MP^{Shh+} but not MP^{Shh-} stimulated NO production in EPC (Figure 4A-B). In addition, the use of the inhibitors cyclopamine and LY 294002 completely prevented the MP^{Shh+}-mediated increase in NO production. As expected, this effect was completely abolished by the presence of the NO synthase inhibitor, L-NAME (Figure 4C-D). Furthermore, MP^{Shh+} treatment had no effect on Akt protein expression nor Akt phosphorylation at its activator site—Ser 473 (Figure 5A). Interestingly, MP^{Shh+} also significantly increased eNOS protein expression and phosphorylation at its activator site (Ser 1177), while MP^{Shh+} treatment reduced eNOS phosphorylation at its inhibitory site (Thr 495; Figure 5B). Cyclopamine and LY 294002 completely abrogated the effects of MP^{Shh+} on the NO pathway in EPC, while in the absence of MP^{Shh+} NO production, protein expression, and Akt and eNOS phosphorylation were unaffected. These results show that MP^{Shh+} activate a SMO and PI3K inhibitor-sensitive mechanism, producing heightened NO production and increased eNOS protein expression and activity.

MP^{Shh+}-mediated capillary-like structure formation is NO-independent

To investigate the relationship between NO production and *in vitro* capillary-like structure formation, EPC were treated with MP^{Shh+} in the presence or absence of L-NAME for 24 hours. Although L-NAME abolished the MP^{Shh+}-induced increase in NO production (Figure 4C-D), it did not affect the increase in the total length of capillary-like structures produced by MP^{Shh+} (Supplementary Figure S3).

MP^{Shh+} effect on cultured EPC isolated from acute myocardial infarction patients

We also cultured EPC isolated from the peripheral blood of patients who had suffered an AMI and tested whether MP^{Shh+} produces similar effects in these cells. The demographic and main clinical data of all participants are presented in Supplemental Table 1. Our results revealed that EPC isolated from patients

that had suffered an acute AMI had a reduced vasculogenic capacity compared to those from healthy volunteers (Figure 6A-B). MP^{Shh+} significantly increased the vasculogenic capacity of healthy donors. Interestingly, MP^{Shh+} also increased the vasculogenic capacity of EPC derived from AMI patients to similar levels to those from healthy donors. In fact, the increase in vasculogenic capacity produced by MP^{Shh+} was indistinguishable between healthy donors (160%) and AMI patients (154%). The effect of MP^{Shh+} in EPC from healthy donors was completely abolished in the presence of cyclopamine. The basal EPC expression of *NOS3*, *VEGFA*, *KDR*, and *KLF2* was not modified in AMI patients (Figure 6C). When cells were exposed to MP^{Shh+} , the expression of these genes in EPC derived from AMI patients increased to the same levels as those from healthy donors. Thus, MP^{Shh+} were able to restore the vasculogenic capacity of EPC obtained from AMI patients.

DISCUSSION

Here, we demonstrate for the first time in human EPC that MP, generated from T lymphocytes under mitogenic and apoptotic conditions and carrying the morphogen Shh, induce: (1) *in vitro* and *in vivo* vasculogenesis; (2) the expression of Shh signaling pathway genes and genes involved in vasculogenesis; (3) NO production which is directly mediated both by the Shh pathway and PI3K activation; and most importantly (4) that MP^{Shh+} improves the vasculogenic capacity of human EPC isolated from AMI patients.

EPC are capable of postnatal vasculogenesis and so are a mechanism for endothelial maintenance and repair because they counteract ongoing endothelial cell injury, replace dysfunctional endothelia, and enhance tissue repair after ischemic vascular injury^{2,24,25}. Among the different EPC sources, human EPC can be isolated and expanded from peripheral blood²³ making them easily to manipulate in laboratory conditions. The cells we isolated here were likely true late EPC, because, in addition to their morphologic characterization (Supplemental figure S1), the EPC obtained using this protocol were positive for the expression of endothelial markers CD31, KDR, CD146, the progenitor marker CD34, and negative for the expression of the panleukocyte marker CD45 (Supplemental figure S2), as previously demonstrated²³.

Revascularization by autologous patient-derived EPC is a promising therapeutic strategy for enhancing vascular repair in ischemic diseases^{26,27} and represents a significantly expanding field²⁸. However, we still lack knowledge of the mechanisms that control EPC function and how this might be augmented.

The use of MP^{Shh+} is one of the most promising developments in the field of cardiovascular medicine and regenerative therapy^{13,21}. Here we demonstrate that MP^{Shh+} can improve the vasculogenic capacity of human EPC *in vitro*, by increasing both the total length and the apparent integrity of EPC-derived tube-like structures. Indeed, this effect is comparable to that previously found for MP^{Shh+} used in human endothelial cells cultured *in vitro*²⁰. The same study also showed that silencing the Shh receptor PTCH1 and pharmacological SMO inhibition with cyclopamine abrogated the effects of MP^{Shh+}, suggesting that its ability to enhance vasculogenesis might be mediated by Hh signaling pathway activation. Accordingly, in two different endothelial cell models, Shh pathway

activation by recombinant Shh induces cyclopamine-sensitive capillary morphogenesis by rapidly activating PI3K and transcriptionally-regulated pathways²⁹.

Our results also indicate that the effect of MP^{Shh+} on EPC *in vitro* is preserved *in vivo* because nude mice implanted with MP^{Shh+}-treated human EPC Matrigel plugs develop more capillaries than controls, **in a Shh-dependent manner**, thus reinforcing the role MP^{Shh+} plays in augmenting vasculogenesis. MP^{Shh+} was previously found to promote neovascularization *in vivo* in a mouse model of hind limb ischemia by stimulating vascular density and blood flow recovery in ischemic limbs after femoral artery ligation²¹. Thus, MP^{Shh+} also improves the vasculogenic function of human EPC isolated from peripheral blood.

In terms of gene expression, our study revealed that *PTCH1*, *SMO*, and *GLI1*, the main members of the Hh signaling pathway, are basally expressed in EPC isolated from peripheral blood samples. Moreover, treating EPC with MP^{Shh+} increases the expression of these genes suggesting activation of the canonical Hh signaling pathway. This concurs with results from Hh-treated bone marrow-derived EPC and primitive human hematopoietic cells^{30,31}. However, HUVEC³² as well as the isolated, expanded, and cultured EPC we used in this study respond differently to Shh. In this sense, it is likely that HUVEC and mature endothelial cells only activate non-canonical responses upon Shh treatment³², while EPC probably activate both canonical and non-canonical responses.

Of note, MP^{Shh+} increases the expression its receptor, SMO. This effect was first demonstrated in *Drosophila*³³ but has also been demonstrated in other experimental models, such as adult motor neurons in rat axotomy³⁴ or in cell hypoxia³⁵, suggesting that Shh may stimulate SMO in an autocrine manner.

In human EPC, MP^{Shh+} induces a cyclopamine-sensitive increase in the mRNA expression of several genes involved in vasculogenesis and NO production, including *VEGF*, *KDR*, *KLF2*, and *eNOS*. This indicates that Shh carried by MP acts on several target genes that regulate vascular function at different levels. Previous studies show that MP^{Shh+} improves endothelial function in the mouse aorta and favors *in vitro*²⁰ and *in vivo* angiogenesis²¹ by increasing NO production through eNOS activity. Surprisingly, inhibition of NO production with

L-NAME does not affect the EPC vasculogenic capacity induced by MP^{Shh+}, suggesting that this effect does not result from MP^{Shh+}-mediated NO production.

Use of the selective inhibitors cyclopamine and LY 294002, completely abrogated the increase in EPC vasculogenic capacity induced by MP^{Shh+}, suggesting that this effect is mainly mediated by mechanisms directly dependent on SMO and PI3K. Our results demonstrate that in EPC, MP^{Shh+} acts via Shh signaling pathway activation and also involves PI3K pathway participation. This mechanism of action is similar to one previously described for endothelial cells treated either with MP^{Shh+20} or with recombinant Shh protein²⁹. However, the ultimate cause of the increase in EPC vasculogenic capacity may also be related to increased VEGFA expression as there is *in vivo* evidence suggesting that the effects of Shh on wound healing are facilitated by increased VEGF-mediated neovascularization and do not result only from stimulating re-epithelialization³⁰. More recently, Renault et al. have shown that Shh-corneal angiogenesis is mediated by activation of the SMO and Rho/ROCK pathways but not by the expression of GLI transcription factors³⁶.

MP^{Shh-}, MP generated under apoptotic conditions and which do not harbor Shh morphogen, have no effect on EPC gene expression, NO production, or vasculogenesis. However, even though these MP do not contain Shh, we cannot exclude the possibility that MP^{Shh+} may contain other proteins not present in MP^{Shh-}, and that this could potentially influence or even potentiate the changes we observed in this study. In fact, MP^{Shh+} can increase the expression of different of proangiogenic factors in endothelial cells^{20,21}, and not all of these factors are regulated in a Shh-dependent manner²¹.

A recent study demonstrated blood outgrowth endothelial cells retain a robust proangiogenic profile with a therapeutic potential for targeting ischemic disease³⁷. In other studies, however, EPC isolated from patients suffering AMI presented a reduced vasculogenic capacity compared to those of EPC isolated from healthy patients. This reinforces evidence that EPC from AMI patients exhibit altered functional behavior, as measured by cell adhesion or calcium influx³⁸. Interestingly, here we demonstrate that MP^{Shh+} treatment can be used to improve the vasculogenesis of EPC derived from AMI patients to levels similar to those found in healthy volunteers, also in a Shh-dependent manner.

In that sense, other authors have recently reported that Shh-modified human CD34 cells preserved cardiac function after infarction through the exosome-mediated delivery of Shh³⁹. Therefore, activating Shh signaling through MP^{Shh+} treatment may rescue cultured EPC function and could potentially be used to promote neovascularization in AMI patients.

In conclusion, our results indicate that MP^{Shh+} exerts a positive effect on EPC by increasing their vasculogenic and NO production capacities **through the Shh pathway**. This effect is maintained in EPC isolated from human peripheral blood samples from patients suffering AMI and in whom both vasculogenic and NO production are impaired. Taken together our results are sufficient to propose the use of MP^{Shh+} and EPC as a potential therapeutic tool for improving vascular regeneration in patients affected by ischemic diseases such as AMI.

FUNDING

This work was supported by the Spanish Ministerio de Economía y Competitividad, Instituto de Salud Carlos III – FEDER-ERDF (grants FIS PI13/00617, FIS PI16/00229, and RD12/0042/0052) and from INSERM and University of Angers (France).

ACKNOWLEDGEMENTS

The authors thank A. Díaz (Central Research Unit of Medicine, University of Valencia) for technical assistance in the *in vivo* Matrigel plug experiments.

CONFLICT OF INTEREST

None declared

REFERENCES

1. Libby P. Fanning the flames: inflammation in cardiovascular diseases. *Cardiovasc Res*. 2015;**107**:307-309.
2. Shantsila E, Watson T, Lip GYH. Endothelial Progenitor Cells in Cardiovascular Disorders. *J Am Coll Cardiol*. 2007;**49**:741-752.
3. Tongers J, Losordo DW, Landmesser U. Stem and progenitor cell-based therapy in ischaemic heart disease: promise, uncertainties, and challenges. *Eur Heart J*. 2011;**32**:1197-1206.
4. Werner N, Junk S, Laufs U, Link A, Walenta K, Böhm M, Nickenig G. Intravenous Transfusion of Endothelial Progenitor Cells Reduces Neointima Formation After Vascular Injury. *Circ Res*. 2003;**93**:e17.
5. Dong C, Goldschmidt-Clermont PJ. Endothelial Progenitor Cells: A Promising Therapeutic Alternative for Cardiovascular Disease. *J Interven Cardiol*. 2007;**20**:93-99.
6. Krenning G, Dankers PYW, Drouven JW, Waanders F, Franssen CFM, van Luyn MJA, Harmsen MC, Popa ER. Endothelial progenitor cell dysfunction in patients with progressive chronic kidney disease. *Am J Physiol - Renal Physiol*. 2009;**296**:F1314-F1322.
7. Tepper OM, Galiano RD, Capla JM, Kalka C, Gagne PJ, Jacobowitz GR, Levine JP, Gurtner GC. Human Endothelial Progenitor Cells From Type II Diabetics Exhibit Impaired Proliferation, Adhesion, and Incorporation Into Vascular Structures. *Circulation*. 2002;**106**:2781.
8. Imanishi T, Hano T, Sawamura T, Nishio I. Oxidized low-density lipoprotein induces endothelial progenitor cell senescence, leading to cellular dysfunction. *Clin Exp Pharmacol Physiol*. 2004;**31**:407-413.
9. Werner N, Nickenig G. Influence of Cardiovascular Risk Factors on Endothelial Progenitor Cells: Limitations for Therapy? *Arterioscler Thromb Vasc Biol*. 2006;**26**:257-266.
10. György B, Szabó TG, Pásztói M, Pál Z, Misják P, Aradi B, László V, Pállinger É, Pap E, Kittel Á, Nagy G, Falus A, Buzás EI. Membrane vesicles, current state-of-the-art: emerging role of extracellular vesicles. *Cell Mol Life Sci*. 2011;**68**:2667-2688.
11. Andriantsitohaina R, Gaceb A, Vergori L, Martínez MC. Microparticles as Regulators of Cardiovascular Inflammation. *Trends Cardiovasc Med*. 2012;**22**:88-92.
12. Martinez MC, Tual-Chalot S, Leonetti D, Andriantsitohaina R. Microparticles: targets and tools in cardiovascular disease. *Trends Pharmac Sci*. 2011;**32**:659-665.
13. Fleury A, Martínez C, Le Lay S. Extracellular vesicles as therapeutic tools in cardiovascular diseases. *Front Immunol*. 2014;**5**:370.
14. Varjosalo M, Taipale J. Hedgehog signaling. *J Cell Sci*. 2007;**120**:3-6.

15. Bailey JM, Singh PK, Hollingsworth MA. Cancer metastasis facilitated by developmental pathways: Sonic hedgehog, Notch, and bone morphogenic proteins. *J Cell Biochem.* 2007;**102**:829-839.
16. Ingham PW, McMahon AP. Hedgehog signaling in animal development: paradigms and principles. *Genes Dev.* 2001;**15**:3059-3087.
17. Robbins DJ, Fei DL, Riobo NA. The Hedgehog Signal Transduction Network. *Sci Signal.* 2012;**5**:re6.
18. Teperino R, Aberger F, Esterbauer H, Riobo N, Pospisilik JA. Canonical and non-canonical Hedgehog signalling and the control of metabolism. *Semin Cell Dev Biol.* 2014;**33**:81-92.
19. Martínez MC, Larbret F, Zobairi F, Coulombe J, Debili N, Vainchenker W, Ruat M, Freyssinet J-M. Transfer of differentiation signal by membrane microvesicles harboring hedgehog morphogens. *Blood.* 2006;**108**:3012-3020.
20. Soleti R, Benameur T, Porro C, Panaro MA, Andriantsitohaina R, Martínez MC. Microparticles harboring Sonic Hedgehog promote angiogenesis through the upregulation of adhesion proteins and proangiogenic factors. *Carcinogenesis.* 2009;**30**:580-588.
21. Benameur T, Soleti R, Porro C, Andriantsitohaina R, Martínez MC. Microparticles Carrying Sonic Hedgehog Favor Neovascularization through the Activation of Nitric Oxide Pathway in Mice. *PLoS ONE.* 2010;**5**:e12688.
22. Agouni A, Mostefai HA, Porro C, Carusio N, Favre J, Richard V, Henrion D, Martinez MC, Andriantsitohaina R. Sonic hedgehog carried by microparticles corrects endothelial injury through nitric oxide release. *FASEB J.* 2007;**21**:2735-2741.
23. Bueno-Betí C, Novella S, Lázaro-Franco M, Pérez-Cremades D, Heras M, Sanchís J, Hermenegildo C. An affordable method to obtain cultured endothelial cells from peripheral blood. *J Cell Mol Med.* 2013;**17**:1475-1483.
24. Berger S, Aronson D, Lavie P, Lavie L. Endothelial Progenitor Cells in Acute Myocardial Infarction and Sleep-disordered Breathing. *Am J Respir Crit Care Med* 2013;**187**:90-98.
25. Grisar JC, Haddad F, Gomari FA, Wu JC. Endothelial progenitor cells in cardiovascular disease and chronic inflammation: from biomarker to therapeutic agent. *Biomark Med.* 2011;**5**:731-744.
26. Moubarik C, Guillet B, Youssef B, Codaccioni J-L, Piercecchi M-D, Sabatier F, Lionel P, Dou L, Foucault-Bertaud A, Velly L, Dignat-George F, Pisano P. Transplanted Late Outgrowth Endothelial Progenitor Cells as Cell Therapy Product for Stroke. *Stem Cell Rev.* 2010;**7**:208-220.
27. Schwarz TM, Leicht SF, Radic T, Rodriguez-Arabaolaza I, Hermann PC, Berger F, Saif J, Böcker W, Ellwart JW, Aicher A, Heeschen C. Vascular Incorporation of Endothelial Colony-Forming Cells Is Essential for Functional Recovery of Murine Ischemic Tissue Following Cell Therapy. *Arterioscler Thromb Vasc Biol.* 2012;**32**:e13-e21.

28. Bianconi V, Sahebkar A, Kovanen P, Bagaglia F, Ricciuti B, Calabrò P, Patti G, Pirro M. Endothelial and cardiac progenitor cells for cardiovascular repair: A controversial paradigm in cell therapy. *Pharmacol Ther.* 2018;**181**:156-168.
29. Kanda S, Mochizuki Y, Suematsu T, Miyata Y, Nomata K, Kanetake H. Sonic Hedgehog Induces Capillary Morphogenesis by Endothelial Cells through Phosphoinositide 3-Kinase. *J Biol Chem.* 2003;**278**:8244-8249.
30. Asai J, Takenaka H, Kusano KF, Ii M, Luedemann C, Curry C, Eaton E, Iwakura A, Tsutsumi Y, Hamada H, Kishimoto S, Thorne T, Kishore R, Losordo DW. Topical Sonic Hedgehog Gene Therapy Accelerates Wound Healing in Diabetes by Enhancing Endothelial Progenitor Cell-Mediated Microvascular Remodeling. *Circulation.* 2006;**113**:2413-2424.
31. Bhardwaj G, Murdoch B, Wu D, Baker DP, Williams KP, Chadwick K, Ling LE, Karanu FN, Bhatia M. Sonic hedgehog induces the proliferation of primitive human hematopoietic cells via BMP regulation. *Nat Immunol.* 2001;**2**:172-180.
32. Chinchilla P, Xiao L, Kazanietz MG, Riobo NA. Hedgehog proteins activate pro-angiogenic responses in endothelial cells through non-canonical signaling pathways. *Cell cycle.* 2010;**9**:570-579.
33. Chen Y, Struhl G. Dual Roles for Patched in Sequestering and Transducing Hedgehog. *Cell.* 1996;**87**:553-563.
34. Akazawa C, Tsuzuki H, Nakamura Y, Sasaki Y, Ohsaki K, Nakamura S, Arakawa Y, Kohsaka S. The Upregulated Expression of Sonic Hedgehog in Motor Neurons after Rat Facial Nerve Axotomy. *J Neurosci.* 2004;**24**:7923-7930.
35. Onishi H, Yamasaki A, Kawamoto M, Imaizumi A, Katano M. Hypoxia but not normoxia promotes Smoothed transcription through upregulation of RBPJ and Mastermind-like 3 in pancreatic cancer. *Cancer Lett.* 2016;**371**:143-150.
36. Renault M-A, Roncalli J, Tongers J, Thorne T, Klyachko E, Misener S, Volpert OV, Mehta S, Burg A, Luedemann C, Qin G, Kishore R, Losordo DW. Sonic hedgehog induces angiogenesis via Rho kinase-dependent signaling in endothelial cells. *J Mol Cell Cardiol.* 2010;**49**:490-498.
37. Dauwe D, Pelacho B, Wibowo A et al. Neovascularization Potential of Blood Outgrowth Endothelial Cells From Patients With Stable Ischemic Heart Failure Is Preserved. *J Am Heart Ass.* 2016;**5**.
38. Rigueiro A, Cuadrado-Godia E, Bueno-Betfí C et al. Mobilization of endothelial progenitor cells in acute cardiovascular events in the PROCELL study: Time-course after acute myocardial infarction and stroke. *J Mol Cell Cardiol.* 2015;**80**:146-155.
39. Mackie AR, Klyachko E, Thorne T, Schultz KM, Millay M, Ito A, Kamide CE, Liu T, Gupta R, Sahoo S, Misener S, Kishore R, Losordo DW. Sonic Hedgehog-Modified Human CD34+ Cells Preserve Cardiac Function After Acute Myocardial Infarction. *Circ Res.* 2012;**111**:312-321.

FIGURE LEGENDS

Figure 1. The capacity of EPC to form capillary-like structures *in vitro* and to induce vasculogenesis *in vivo*. EPC isolated from peripheral blood samples from healthy patients were incubated for 24 hours on a Matrigel matrix, either in the presence or in the absence of 10 µg/mL MP^{Shh+} or 10 µg/mL MP^{Shh-}. (A) Representative phase-contrast images of capillary-like structures. (B) Quantification of the total length of capillary structures. Data are expressed as mean ± SEM (each point is the average of five random fields, n = 6 independent experiments). In another set of experiments, EPC in culture were treated or without 10 µg/mL MP^{Shh+} for 24 hours, either in the presence or absence of 15 µM cyclopamine. After treatment, 7.5 × 10⁵ EPC were mixed with 300 µL Matrigel reagent and injected subcutaneously into nude RjOrl:NMRI-Foxn1nu/Foxn1nu mice. (C) Representative macroscopic images of Matrigel plugs, 7 days after subcutaneous injection. (D) Total hemoglobin content per plug relative to the control values, expressed as mean ± SEM (n = 3-6 plugs). For quantitative analysis of angiogenesis and blood vessel architecture, EPC were visualized with green CD31 and red CD34 immunofluorescence. Nuclei were counterstained with DAPI (blue). (E) Representative images of vascular network formation in the Matrigel plug 7 days after implantation at 100× magnification are shown. (F) The relative quantity of CD31⁺ (closed symbols) and CD34⁺ (open symbols) EPC was estimated by calculating the area occupied by green and red fluorescence (pixels), respectively. Data are the mean values ± SEM (each point is the average of five random fields, n = 3 independent experiments). *p < 0.05, **p < 0.01, and ***p < 0.001.

Figure 2. Gene expression in EPC treated with MP. EPC were incubated either in the presence of 10 µg/mL MP^{Shh+} or 10 µg/mL MP^{Shh-} for 24 hours. After treatment, expression of *PTCH1*, *SMO*, *GLI1*, *NOS3*, *VEFG*, *KDR*, and *KLF2* was determined by real time quantitative PCR. (A) Shh signaling pathway gene expression. (B) Expression of genes of cardiovascular interest. Data are the mean ± SEM (n = 3–5 independent experiments, performed in different cell cultures). *p < 0.05, **p < 0.01, and ***p < 0.001.

Figure 3. *In vitro* EPC capillary-like structure formation and Shh signaling pathways. EPC were incubated either in the presence of 10 µg/mL MP^{Shh+} or 10 µg/mL MP^{Shh-} for 24 hours, preincubated or without 15 µM cyclopamine or 10 µM LY 294002, on a Matrigel matrix. (A) Representative phase-contrast images of capillary-like structures. (B) Quantification of the total length of capillary-like structures relative to the control values. Data are the mean ± SEM (each point is the average of five random fields, n = 4–10 independent experiments). *p < 0.05, **p < 0.01, and ***p < 0.001.

Figure 4. NO production induced by MP on EPC. To evaluate the involvement of the Shh signaling pathway in NO production, EPC were incubated in the presence or absence of 10 µg/mL MP^{Shh+} or 10 µg/mL MP^{Shh-} for 24 hours, pre-incubated or without 15 µM cyclopamine or 10 µM LY 294002. Cells were then loaded with the fluorescent probe DAF-FM diacetate to determine total NO-production (A) Representative fluorescence images of NO production by treated EPC. (B) Quantification of total NO production relative to the control values, is presented as mean ± SEM (n = 4–10 independent experiments, performed in different cell cultures). In another set of experiments, EPC were incubated for 24 hours in the presence or absence of 10 µg/mL MP^{Shh+}, pre-incubated or without 100 µM of the NO synthase inhibitor L-NAME, and NO production was tested. (C) Representative images of NO production by cultured EPC after different treatments. (D) Total NO production quantification, relative to the control values, is expressed as the mean ± SEM (n = 5 independent experiments, performed in different cell cultures). ***p < 0.001.

Figure 5. Regulation of NO production and the Shh signaling pathway. EPC were incubated in the presence or in the absence of 10 µg/mL MP^{Shh+} or 10 µg/mL MP^{Shh-} for 24 hours, pre-incubated or without 15 µM cyclopamine or 10 µM LY 294002. Representative western blot images and relative levels assessed by densitometry showing the effect of MP treatment on (A) total Akt and phosphorylation of Akt at Serine 473 (presented as the ratio of total and

phosphorylated protein) and (B) total eNOS expression and phosphorylation of eNOS at Serine 1177 and Threonine 495 (both presented as the ratio of total and phosphorylated protein). Data are the mean \pm SEM (n = 3–7 independent experiments, performed in different cell cultures). *p < 0.05, **p < 0.01, and ***p < 0.001.

Figure 6. The effect of MP on EPC isolated from acute myocardial infarction patients. EPC were isolated from peripheral blood samples from healthy donors (HD) and acute myocardial infarction patients (AMI). EPC were incubated for 24 hours either in the presence or in the absence of 10 μ g/mL MP^{Shh+}, preincubated or without 15 μ M cyclopamine, on a Matrigel matrix. (A) Representative phase-contrast images of capillary-like structures. (B) Total length quantification of capillary structures formed on the Matrigel matrices were expressed relative to healthy donor values as the mean \pm SEM (each point is the average of five random fields, n = 5–11 independent experiments). (C) After treatment, expression of genes of cardiovascular interest (*NOS3*, *VEFG*, *KDR*, and *KLF2*) was determined by real time quantitative PCR. Data are the mean \pm SEM (n = 7–8 independent experiments, performed in different cell cultures). *p < 0.05, **p < 0.01, and ***p < 0.001.

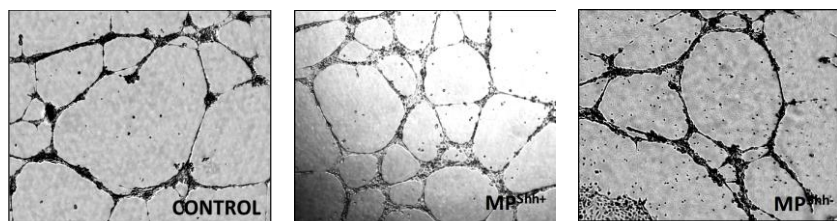
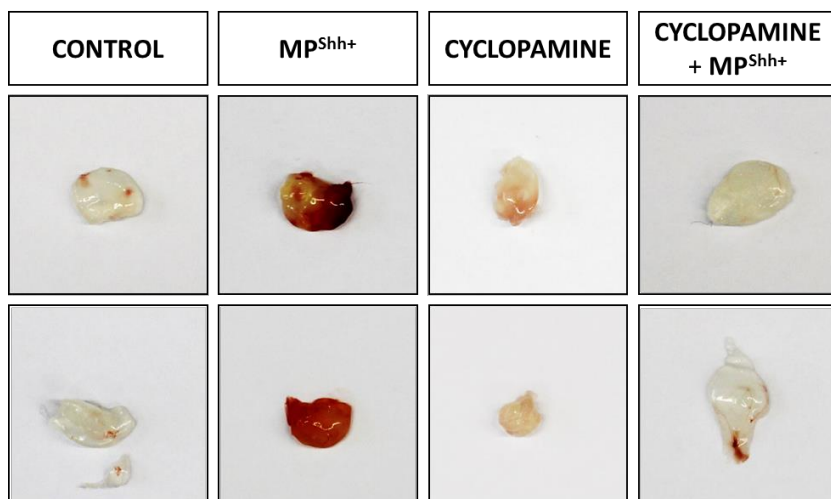
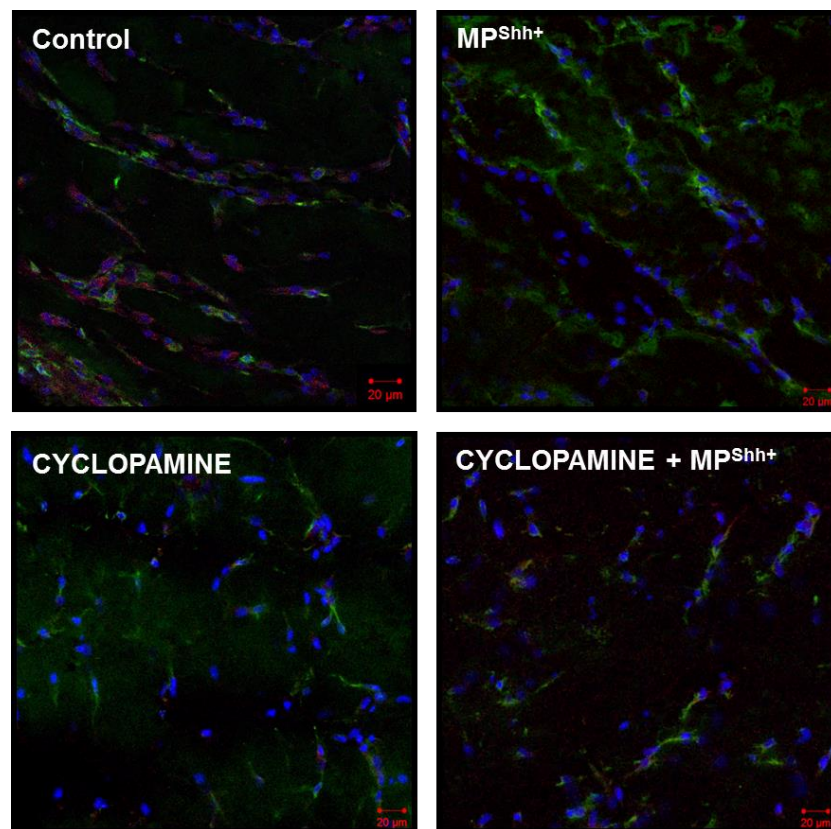
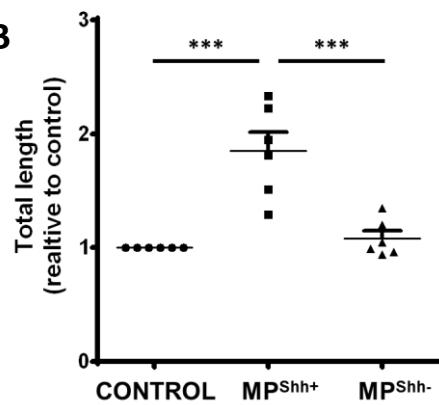
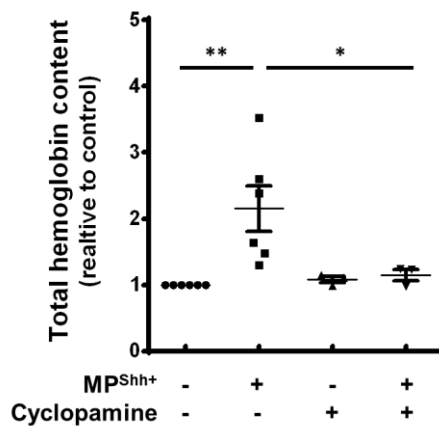
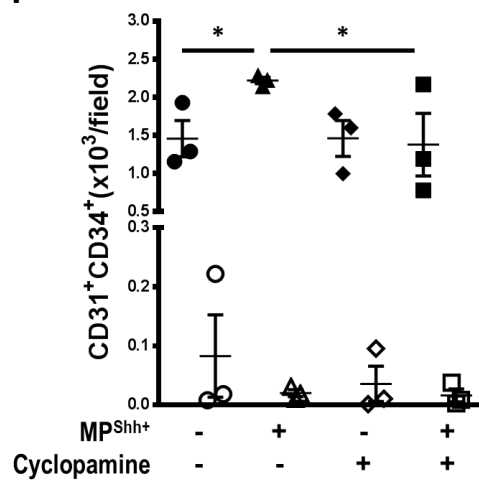
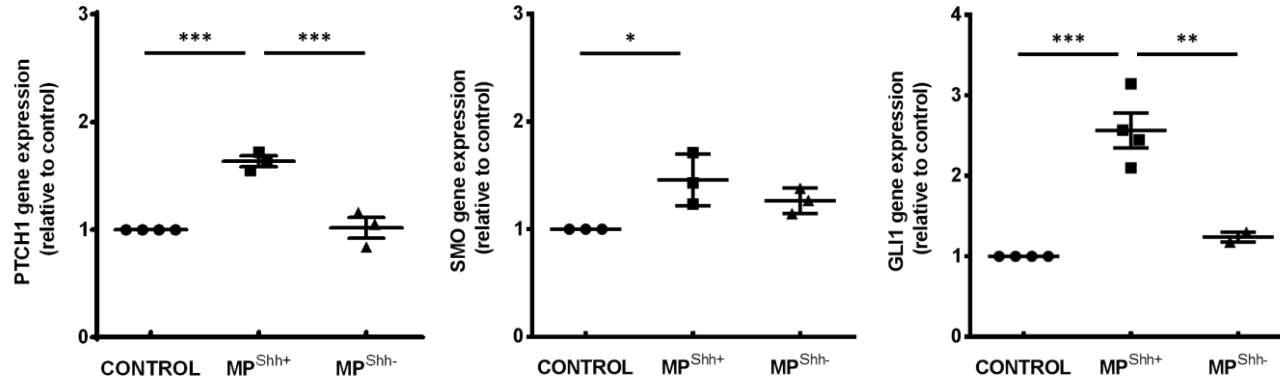
FIGURE 1**A****C****E****B****D****F**

Figure 2
FIGURE 2

A



B

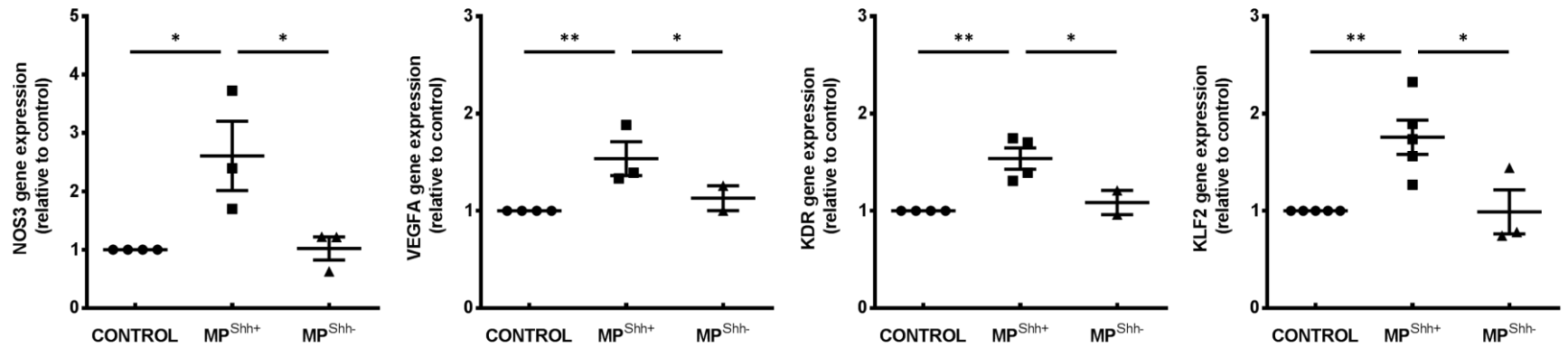
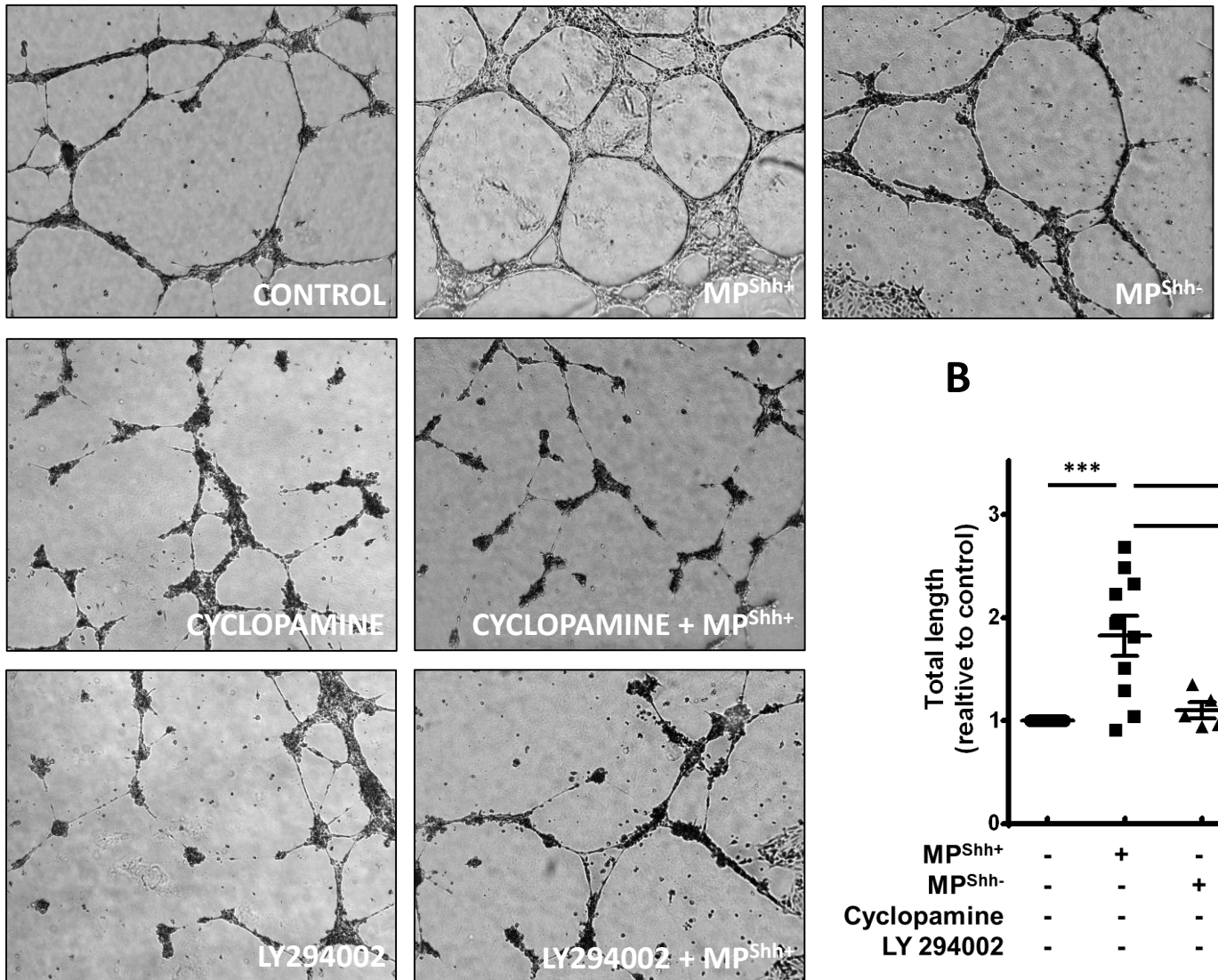


FIGURE 3

A



B

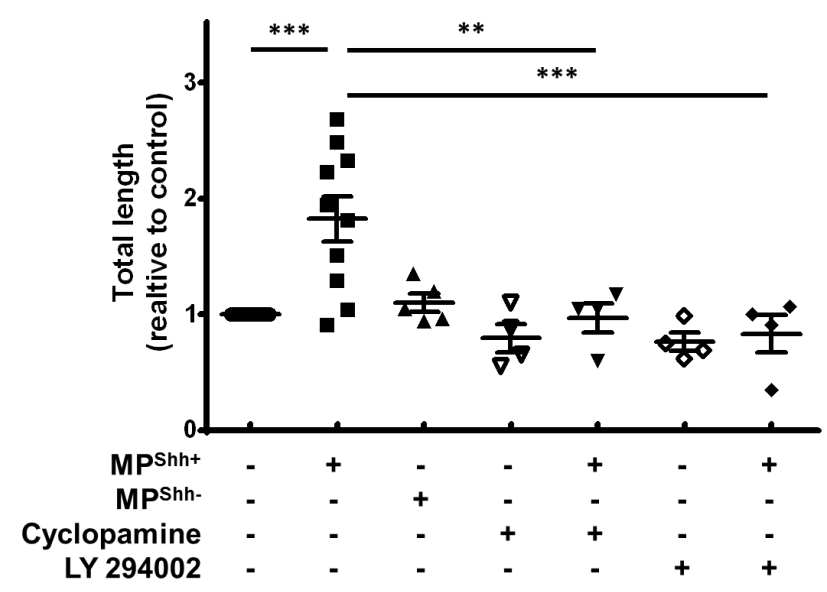
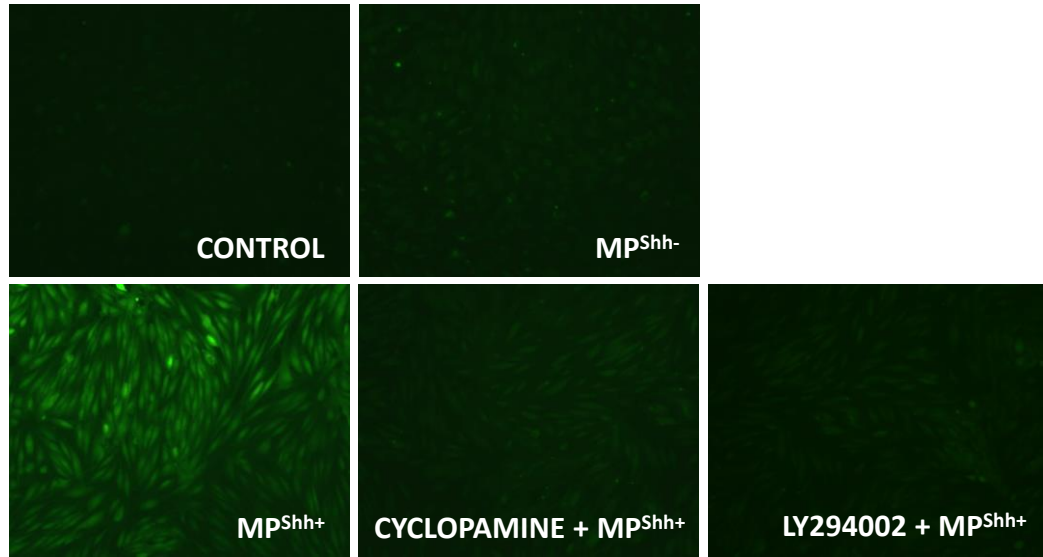
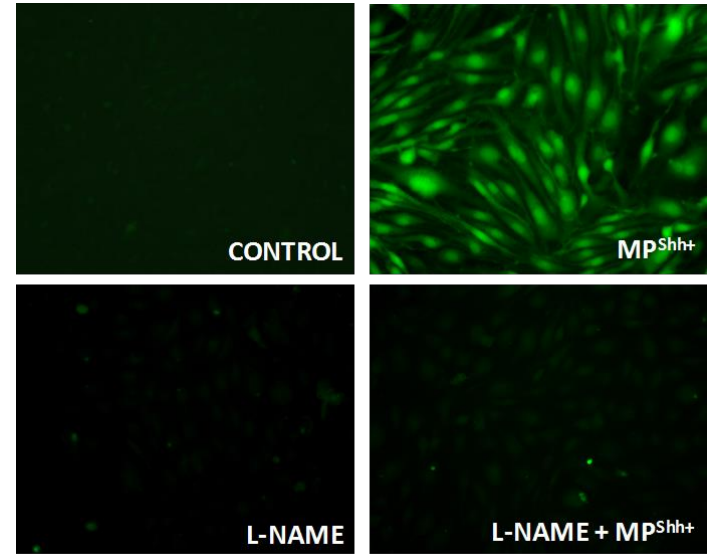


Figure 4

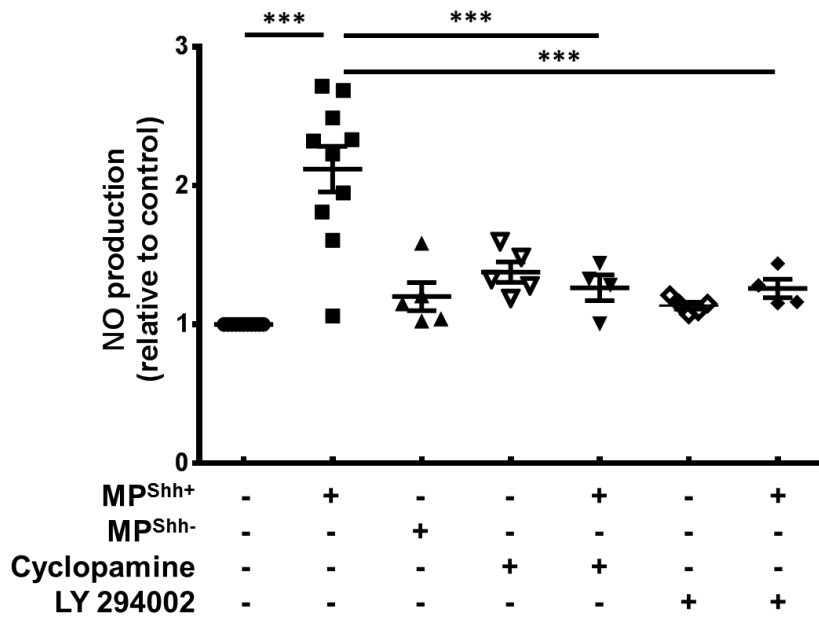
A



C



B



D

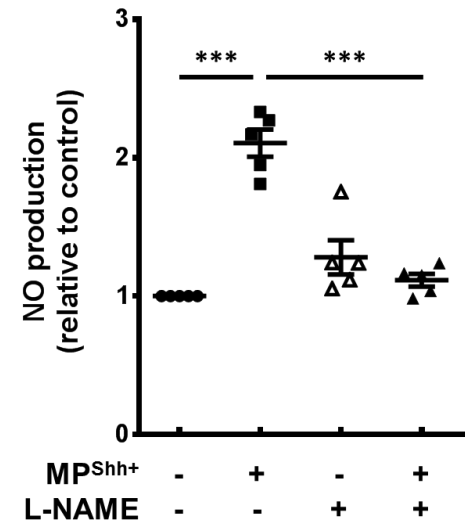
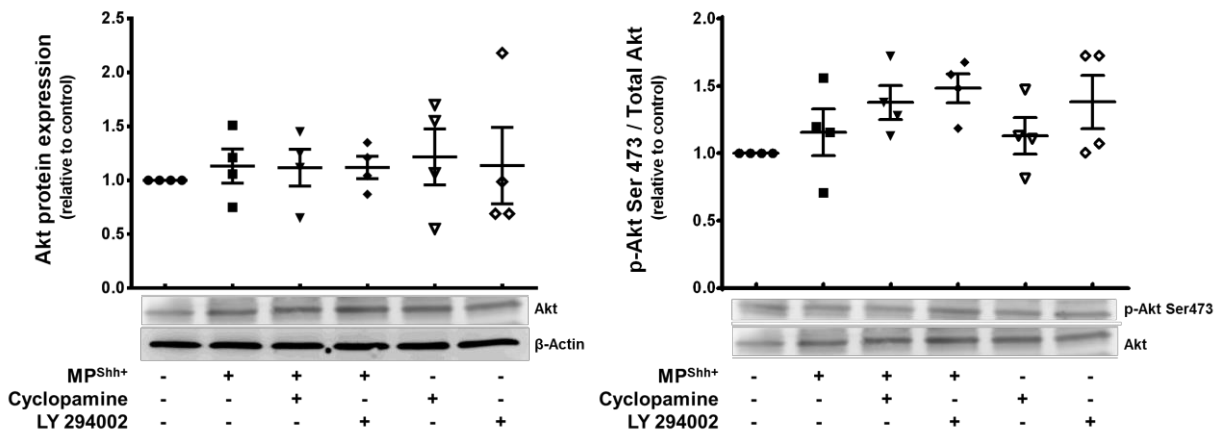


Figure 5

FIGURE 5

A



B

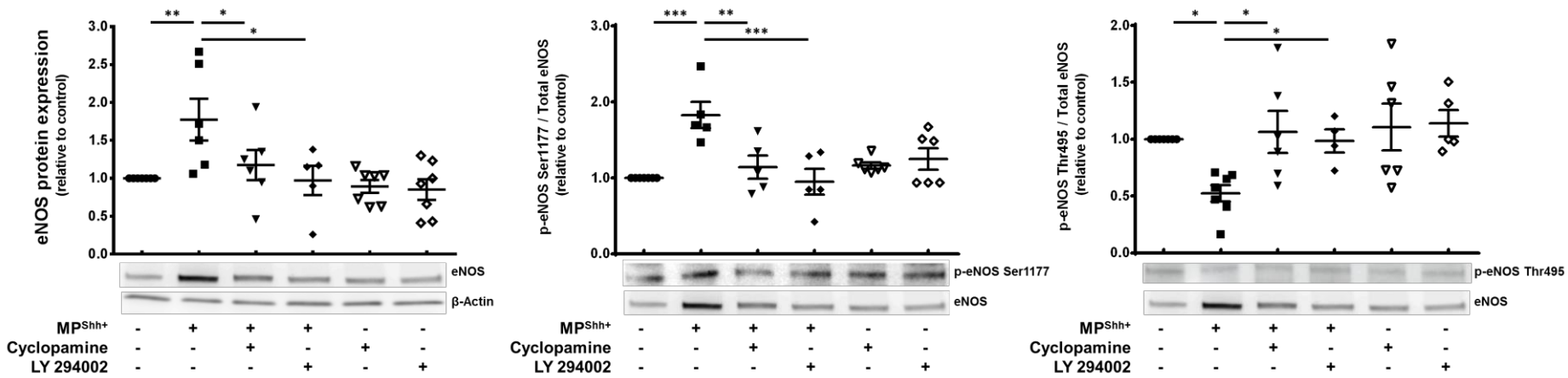
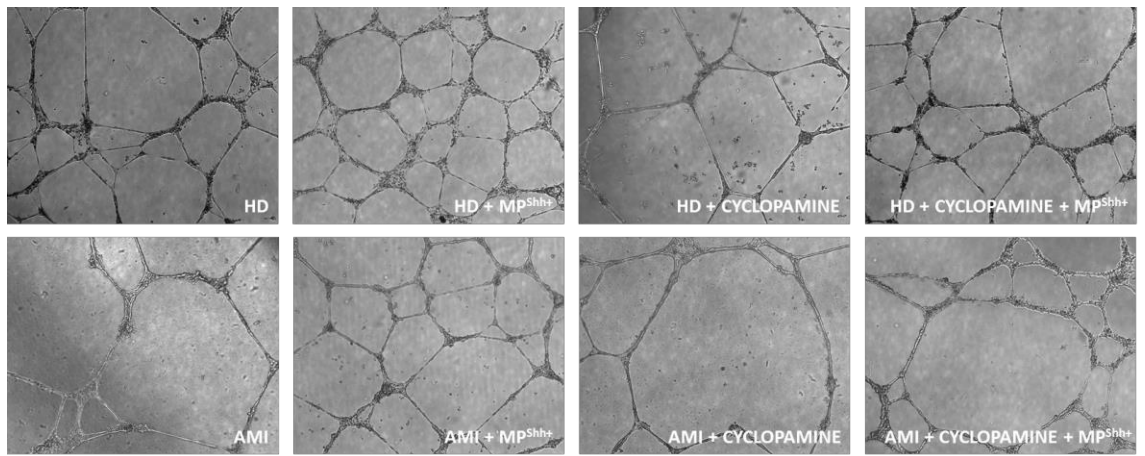
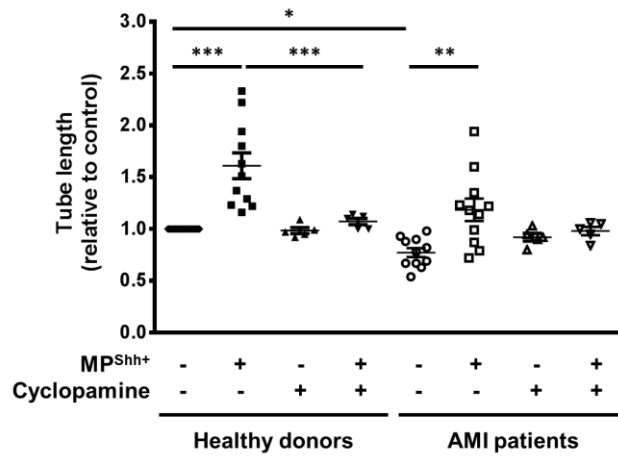
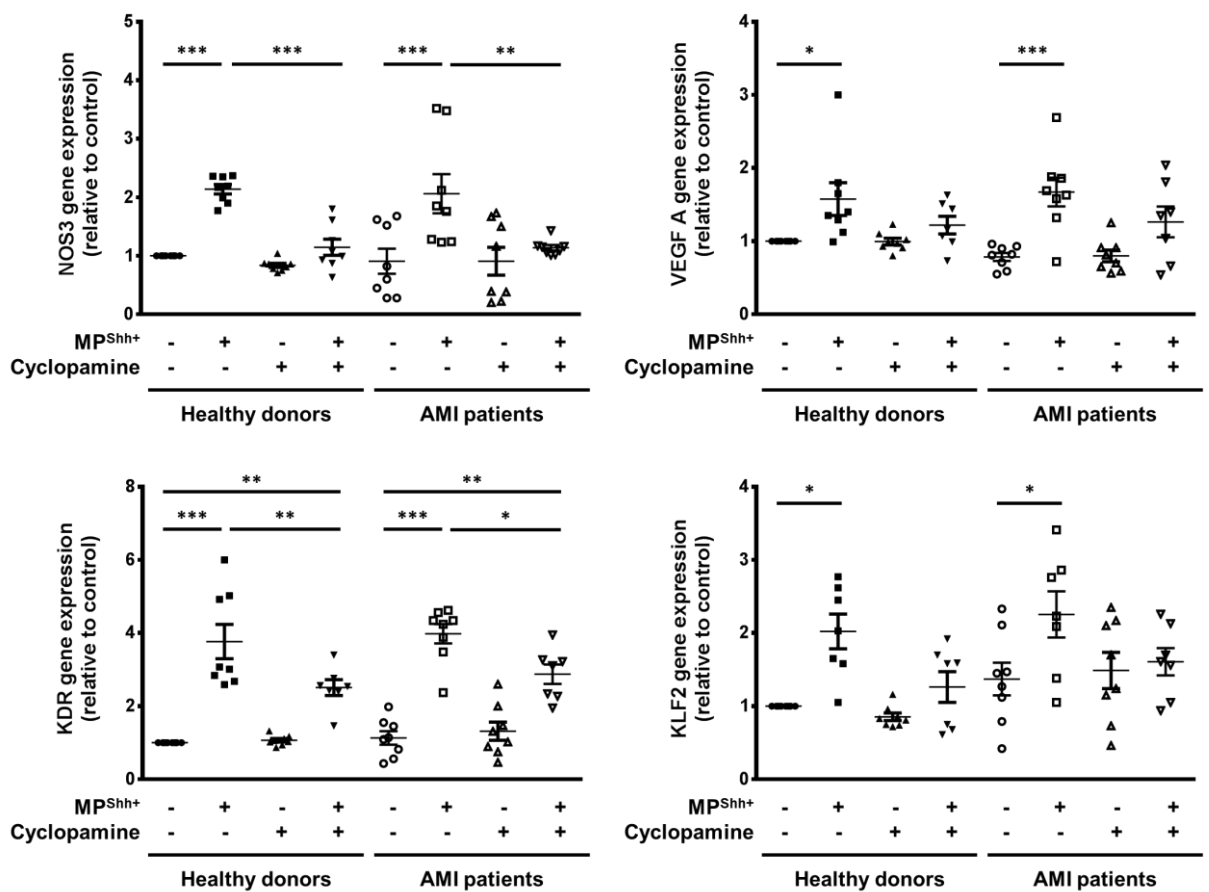


FIGURE 6**A****B****C**

SUPPLEMENTARY MATERIAL:

**MICROPARTICLES HARBORING SONIC HEDGEHOG MORPHOGEN
IMPROVE THE VASCULOGENESIS CAPACITY OF ENDOTHELIAL
PROGENITOR CELLS DERIVED FROM MYOCARDIAL INFARCTION
PATIENTS**

Authors: C. Bueno-Betí, S. Novella, R. Soletí, A. Mompeón, L. Vergori, J. Sanchís, R. Andriantsitohaina, M.C. Martínez, C. Hermenegildo

MATERIAL AND METHODS

This investigation conforms to the principles outlined in the Declaration of Helsinki, was approved by the INCLIVA clinical research Ethical Committee, and written informed consent was obtained from all donors. The animal studies were carried out using approved protocols by the Institutional Ethics Committee at the University of Valencia, conformed to the National Institutes of Health Guide for the Care and Use of Laboratory Animals.

EPC isolation, culture and characterization

EPC isolation and culture was performed as previously described in detail by our group ¹. Concisely, 30 mL of peripheral blood were withdrawn from healthy subjects (n=20) and from diagnosed patients with acute myocardial infarction (n=11). Then, mononuclear cells (MNC) were isolated by density gradient centrifugation (Lymphoprep, Axis-shield, Oslo, Norway). Once isolated, MNC were seeded onto fibronectin-treated culture dishes (2.5 µg/cm²; Becton Dickinson, Madrid, Spain) in complete EGM-2 culture medium (Lonza, Cultek, Barcelona, Spain) supplemented with 20% fetal bovine serum (FBS) (Life technologies, Alcobendas, Spain). After 24 hours of culture, non-adherent cells were removed and those that remained attached were further cultured at 37°C and 5% of CO₂ until first cobble stone-like EPC colonies appeared. Cultures were replaced with fresh media every two days.

The endothelial nature of isolated EPC cultures was determined by measuring their ability to uptake acetylated low density lipoprotein (acLDL), to bind Ulex-lectin and to express von Willebrand Factor (vWF). EPC were incubated with Dil-acLDL (Life Technologies, Alcobendas, Spain) for 4 hours at 37°C. Then, EPC cultures were fixed with 4% paraformaldehyde and incubated with fluorescein isothiocyanate labelled Ulex lectin agglutinin (FITC-UEA-1, Sigma-Aldrich). For vWF expression, EPC were fixed and permeabilized and incubated with rabbit polyclonal vWF antibody (Cat#: ab6994; Abcam, Cambridge, United Kingdom) and then with a DyLight 488 conjugated anti-rabbit secondary antibody (Cat#: ab96919; Abcam). Counter staining was achieved by incubating cells with 4,6-diamidino-2-phenylindole (DAPI, Sigma-Aldrich). Images were acquired with an inverted fluorescence microscope Nikon Eclipse Ti.

Microparticle preparation

MP were generated from human lymphoid CEM T cell line (ATCC, Manassas, VA, USA) as previously described^{2,3}. Cells were seeded at density of 10^6 cells/mL, cultured in serum-free XIVO 15 medium (Lonza). For the production of MP^{Shh+}, CEM T cells were treated with phytohaemagglutinin (10 µg/mL; Sigma-Aldrich, Tres Cantos, Madrid, Spain) for 72 hours, with phorbol-12-myristate-13 (40 ng/mL; Sigma-Aldrich) and actinomycin D (1 µg/mL; Sigma-Aldrich) for 24 hours. For the production of MP not harboring Shh morphogen (MP^{Shh-}), CEM T cells were treated only with actinomycin D (0.5 µg/mL) for 24 hours.

After treatment, culture supernatant was recovered and two centrifugation steps at 750 x g for 15 minutes and at 1500 x g for 5 minutes to remove cells and large debris were performed. Remaining MP-containing supernatant was subjected at 14,000 x g for 45 minutes to pellet MP. Pelleted MP were washed twice in sterile NaCl (0.9% w/v) by two series of centrifugations at 14,000 x g for 45 minutes. Finally, MP were recovered in 400 µL sterile NaCl (0.9% w/v). MP content was adjusted to protein content determined against bovine serum albumin (BSA) standards to contain 10 µg proteins per mL. Both MP^{Shh+} and MP^{Shh-} were used at concentration of 10 µg/mL which is the maximal effective concentration previously found able to induce angiogenesis^{3,4}.

Formation of capillary-like structures *in vitro*

EPC isolated from peripheral blood samples were seeded on 24-well plates coated with Matrigel® (Becton Dickinson) as specified by manufacturer. Briefly, Matrigel substrate was diluted with serum-free EGM-2 medium (1:1 dilution) and 200 µL were added into a 24-well plate and allowed to solidify for 1 hour at 37°C. Afterwards, 1.5×10^5 cells/well were incubated with EGM-2 medium containing 2% of FBS and allowed to adhere for 1 hour. Then, cells were incubated for 24 hours either in the presence or in the absence of MP^{Shh+} (10 µg/mL) or MP^{Shh-} (10 µg/mL). In some experiments, the SMO inhibitor cyclopamine (15 µM; Sigma-Aldrich) or PI3K inhibitor LY 294002 (10 µM; Calbiochem, London, UK) were added 30 minutes before starting the treatment with MP. The desired concentrations of cyclopamine and LY294002 were obtained by successive dilutions of a stock solution with DMSO. Control cells were exposed to 1% DMSO to discard any effect of vehicles. Capillary-like structure formation was recorded by Nikon digital sight Ds-QiMc camera and

Nikon Eclipse-Ti inverted microscope (Nikon, Izasa, Valencia, Spain) with 4X objective (total magnification 40X). For each experimental condition, five random fields were selected and analyzed with Image Pro-Plus Software V.6 (Media Cybernetics, Rockville, USA). All measurements were conducted by an observer blinded to the experimental group assignment.

***In vivo* Matrigel plug assay**

For *in vivo* studies of MP-induced EPC vasculogenesis, EPC were incubated in absence or in presence of MP^{Shh+} (10 µg/mL), either in the presence or absence of 15 µM cyclopamine, for 24 hours *in vitro*. Matrigel reagent was supplemented with growth factors contained in EGM-2 single quotes. Matrigel plugs were prepared on ice by mixing 300 µL of Matrigel with 7.5×10^5 EPC, pretreated or not with MP^{Shh+}. Thereafter, Matrigel plugs were subcutaneously injected on each hind flank of nude RjOri:NMRI-Foxn1nu/Foxn1nu mice under isoflurane anaesthesia (n=6 controls, n=6 MP^{Shh+}, n=3 cyclopamine and n=6 cyclopamine + MP^{Shh+}). Animals health were daily monitored by specialized supervisors. After 7 days, mice were euthanized under isoflurane anaesthesia. Right hind flank plugs were removed and homogenized in lysis buffer (17mM Tris HCl, 0.75% NH₄Cl pH 7.6) overnight at 4°C. Total hemoglobin content per plug, referred to its weight, was determined by Drabkin's reagent (Sigma-Aldrich). Left hind flank plugs were removed and directly frozen in OCT embedding compound (Tissue-Tek, Sakura Finetek Spain, Barcelona, Spain) for immunohistochemistry.

Immunohistochemistry of Matrigel plugs

Frozen Matrigel plugs sections (20 µm thickness) were prepared using a Leica CM3050S cryostat (Leica, Rueil-Malmaison, France) and then briefly fixed with 4% PFA. Slides were incubated for 90 min at room temperature in blocking buffer (5% bovine serum in PBS) to block nonspecific antibody binding. Sections were then treated for overnight at 4 °C with primary mouse anti-human CD31 antibody (Cat#: 89C2; Cell Signaling Technology, Danvers, MA, USA; dilution 1:1000). Following washing steps with PBS, sections were treated with rabbit anti-human CD34 (Cat#: NBP2-38322; Novus Biologicals, Abingdon, United Kingdom; dilution 1µg/ml), in the dark for 90min at room temperature. Following three washes with PBS, either Alexa Fluor 488 goat anti-mouse (Cat#: A-11001; Molecular Probes, Eugene, OR, USA, dilution 2µg/ml) and goat

anti-rabbit Alexa Fluor 546 (Cat#: FP-SB5000 Interchim, Montluçon, France, dilution 1:1000), secondary antibodies, were applied to detect CD31 and CD34, respectively. Nuclei were counterstained with 4,6-diamidino-2-phenylindole (DAPI) (Santa Cruz Biotechnology, Heidelberg, Germany) at room temperature for 5 minutes. Confocal microscopy and digital image recording were used. Then we calculated the vessel area in each category using ImageJ software (National Institute of Health, USA).

Quantitative Polymerase Chain Reaction analysis

To determine the expression of Shh pathway signaling genes and genes of cardiovascular interest on EPC, cells were incubated for 24 hours either in the presence or in the absence of MP^{Shh+} (10 µg/mL) or MP^{Shh-} (10 µg/mL). Then, cells were washed twice in DPBS and recovered in TRIzol® Reagent (Life Technologies) following the manufacturer instructions. Total RNA isolation was performed by using PureLink® RNA Mini Kit (Life Technologies). For reverse transcription reactions, 300 ng of total RNA was reverse transcribed using the High-Capacity cDNA reverse transcription kit (Applied Biosystems, Foster City, CA, USA) according to the manufacturer's instructions. The mRNA levels were determined by quantitative real-time PCR analysis using an ABI Prism 7900 HT Fast Real-Time PCR System (Applied Biosystems).

Gene-specific primer pairs and probes for *PTCH1* (Hs00181117_m1, Assay-on-Demand, Applied Biosystems), *SMO* (Hs01090242_m1, Assay-on-Demand, Applied Biosystems), *GLI1* (Hs01110766_m1, Assay-on-Demand, Applied Biosystems), *NOS3* (Hs01574659_m1, Assay-on-Demand, Applied Biosystems), *VEGFA* (Hs00900054_m1, Assay-on-Demand, Applied Biosystems), *KDR* (Hs00176676_m1, Assay-on-Demand, Applied Biosystems) and *KLF2* (Hs00360439_g1, Assay-on-Demand, Applied Biosystems) were used together with TaqMan Universal PCR Master Mix (Applied Biosystems) and reverse-transcribed RNA samples in 20-µL reaction volumes. Each sample was analyzed in triplicates, and the expression values were calculated according to the $2^{-\Delta\Delta C_t}$ method.

Determination of nitric oxide production

NO production on cultured EPC was determined by using 4-amino-5-methylamino- 2',7'-difluorofluorescein diacetate (DAF-FM diacetate) fluorescent probe (Life technologies) following manufacturer instructions. Firstly, cells were

incubated for 24 hours either in the presence or in the absence of MP^{Shh+} (10 µg/mL) or MP^{Shh-} (10 µg/mL) preincubated or not with cyclopamine (15 µM), LY 294002 (10 µM) or NO synthase inhibitor N ω -Nitro-L-arginine methyl ester hydrochloride (L-NAME, 100 µM). The desired concentrations of cyclopamine and LY294002 were obtained by successive dilutions of a stock solution with DMSO, and L-NAME was diluted in distilled water. Control cells were exposed to 1% DMSO to discard any effect of vehicles. After treatment, DAF-FM diacetate (3.8 µM) was added to the culture media and further incubated for 30 minutes at 37°C and 5% of CO₂. DAF-FM diacetate was removed by two washing steps with DPBS (Life technologies). Then fresh medium with the corresponding treatments was added and cells were further incubated for 15 minutes to allow complete de-esterification of the intracellular diacetates. NO production was determined by measuring DAF-FM fluorescence on Nikon digital sight Ds-QiMc camera and Nikon Eclipse-Ti fluorescence inverted microscope (with 10X objective; total magnification 100X). For each experimental condition, five random fields were analyzed with Image Pro-Plus Software V.6 and the mean intensity fluorescence per power field was recorded.

Western blot analysis

To evaluate the expression levels of proteins involved in NO production, EPC cultures were incubated for 24 hours either in the presence or in the absence of MP^{Shh+} (10 µg/mL) or MP^{Shh-} (10 µg/mL), preincubated or not with cyclopamine (15 µM) or LY 294002 (10 µM) for 30 minutes. The desired concentrations of cyclopamine and LY294002 were obtained by successive dilutions of a stock solution with DMSO. Control cells were exposed to 1% DMSO to discard any effect of vehicles. Then, EPC cultures were recovered in RIPA buffer (Sigma, Tres Cantos, Madrid, Spain) containing protease inhibitors (Complete ULTRA Tablets, Roche Diagnostics, Madrid, Spain) and phosphatase inhibitors (PhosStop Tablets, Roche Diagnostics). Equal amounts of protein were separated in 6.5% SDS–Polyacrylamide gel by electrophoresis and then transferred to PVDF sheets (PVDF Transfer Membrane, Bio-Rad, Madrid, Spain).

Membranes were incubated overnight at 4°C with 1:500 dilution of the following primary antibodies: Akt (Cat#: 9272; Cell Signaling Technology), phospho-Akt (Ser 473) (Cat#: 9271; Cell Signaling Technology), eNOS (Cat#: sc-654; Santa

Cruz Biotechnology), phospho-eNOS (Ser 1177) (Cat#: 9571; Cell Signaling Technology) and phospho-eNOS (Thr 495) (Cat#: 9574; Cell Signaling Technology). Densitometric analyses of Western blots were performed using MacBiophotonic ImageJ software. All membranes were re-blotted using a monoclonal antibody against β -actin (Cat#: A-5441; 1:5000; Sigma-Aldrich) as loading control. Data were normalized to corresponding values of β -actin densitometry.

Statistical analysis

Data normality was assessed by Kolmogorov-Smirnov test. Values shown in the text and figures represent the mean \pm Standard Error of the Mean (SEM). Statistical analysis was performed by using either Student's t-test for single comparisons or one-way analysis of variance (ANOVA) for multiple comparisons and Newman-Keuls post-test. P values <0.05 were considered significant. Statistical analysis was carried out by using Prism 5.04 software (GraphPad Software Inc., San Diego, CA, USA).

References

1. Bueno-Betí C, Novella S, Lázaro-Franco M, Pérez-Cremades D, Heras M, Sanchís J, Hermenegildo C. An affordable method to obtain cultured endothelial cells from peripheral blood. *J Cell Mol Med*. 2013;**17**:1475-1483.
2. Agouni A, Mostefai HA, Porro C, Carusio N, Favre J, Richard V, Henrion D, Martínez MC, Andriantsitohaina R. Sonic hedgehog carried by microparticles corrects endothelial injury through nitric oxide release. *FASEB J*. 2007;**21**:2735-2741.
3. Soleti R, Benameur T, Porro C, Panaro MA, Andriantsitohaina R, Martínez MC. Microparticles harboring Sonic Hedgehog promote angiogenesis through the upregulation of adhesion proteins and proangiogenic factors. *Carcinogenesis*. 2009;**30**:580-588.
4. Benameur T, Soleti R, Porro C, Andriantsitohaina R, Martínez MC. Microparticles Carrying Sonic Hedgehog Favor Neovascularization through the Activation of Nitric Oxide Pathway in Mice. *PLoS ONE*. 2010;**5**:e12688.

Supplemental TABLE 1

Variable	CONTROL	AMI patients	p
Demographic data			
Men	8 (73 %)	9 (82 %)	-
Age (years)	56.3 ± 3.2	50.4 ± 2.2	-
Body mass index	24.8 ± 0.5	27.5 ± 1.5	0.090
Clinical data			
Systolic blood pressure (mmHg)	122.1 ± 3.3	138.1 ± 9.7	0.121
Diastolic blood pressure (mmHg)	74.5 ± 2.3	86.4 ± 7.1	0.113
Heart rate (bpm)	67.5 ± 1.7	76.6 ± 4.6	0.072
Total cholesterol (mg/dL)	180.8 ± 5.2	200.5 ± 9.3	0.073
LDL (mg/dL)	110.3 ± 4.7	123.7 ± 7.9	0.155
HLD (mg/dL)	53.2 ± 2.7	46.4 ± 3.5	0.135
Triglycerides	90.0 ± 8.8	151.0 ± 29.9	0.055
Diabetes	-	-	-
Smoking	1 (9 %)	4 (36 %)	-
Treatment			
Acetylsalicylic acid	-	11 (100 %)	-
Clopidogrel	-	8 (73 %)	-
ACEI/ARB	-	10 (91 %)	-
Beta-blockers	-	9 (82 %)	-
Statins	-	11 (100 %)	-

Data expressed as n (%) or mean ± SEM

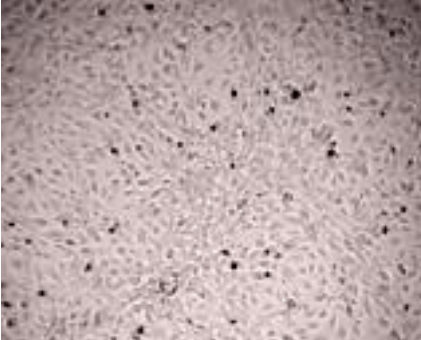
Supplementary Figures for:

MICROPARTICLES HARBORING SONIC HEDGEHOG MORPHOGEN IMPROVE THE VASCULOGENESIS CAPACITY OF ENDOTHELIAL PROGENITOR CELLS DERIVED FROM MYOCARDIAL INFARCTION PATIENTS

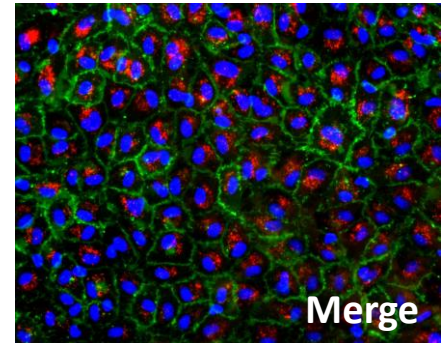
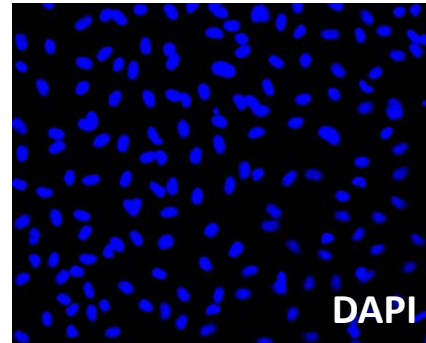
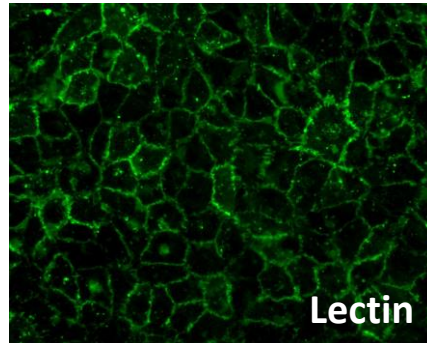
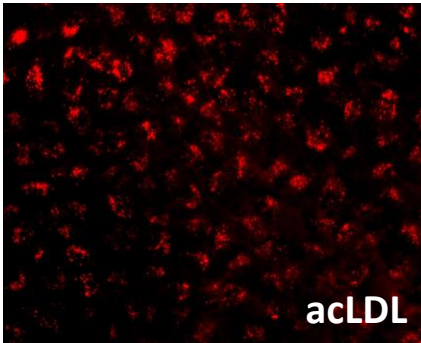
Authors: C. Bueno-Betí, S. Novella, R. Soletí, A. Mompeón, L. Vergori, J. Sanchís, R. Andriantsitohaina, M.C. Martínez, C. Hermenegildo

FIGURE S1

A



B



C

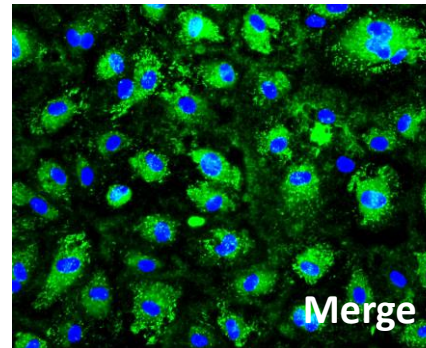
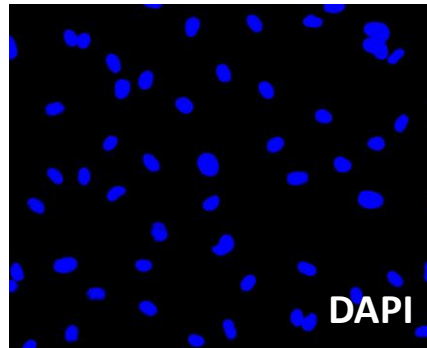
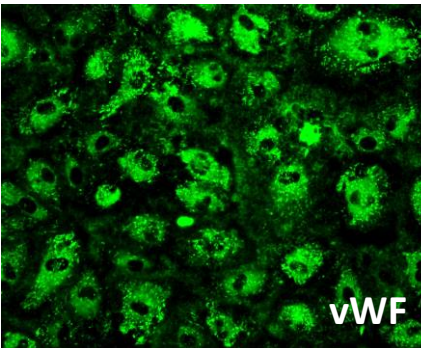


Figure S1. EPC morphology and phenotypic characterization. (A) Cobblestone-like morphology of isolated EPC cultured at 37°C and 5% CO₂. (B) Representative fluorescence microscopy images of EPC ability to uptake acetylated LDL uptake, Lectin binding, (C) vWF expression, nuclei counterstaining with DAPI and merged images. Images were obtained with Nikon Eclipse-Ti inverted microscope 4X objective for (A), 10X objective for (B) and 20X objective for (C) (total magnification 40X, 100X and 200X, respectively) (n = 5, independent experiments, performed in different cell cultures).

FIGURE S2

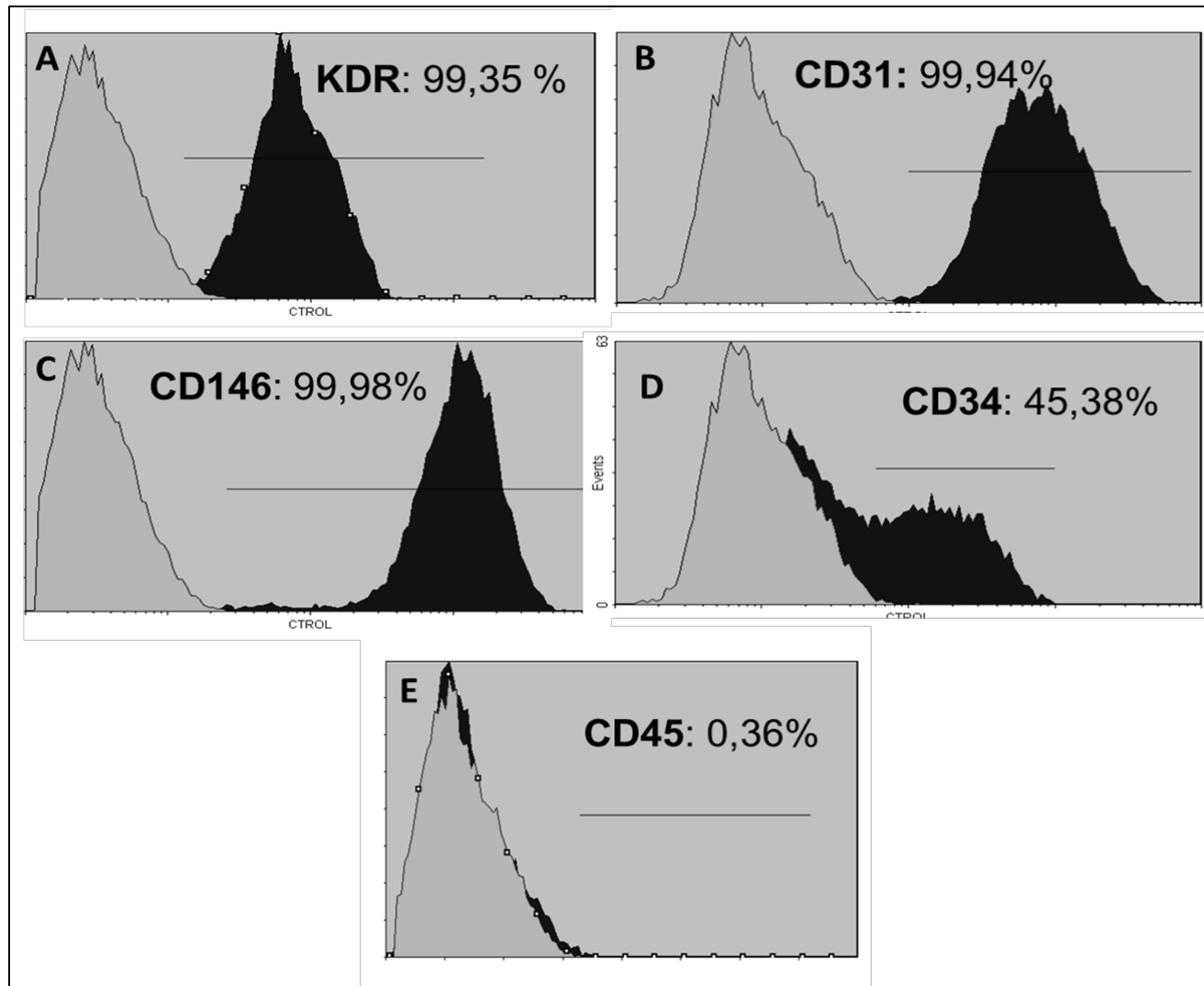


Figure S2. EPC immunophenotypic characterization. Representative images for endothelial markers kinase insert domain receptor (KDR), CD31 and CD146, the progenitor maker CD34 and the leucocyte antigen CD45. The expression were assessed by flow cytometry. Grey histograms are isotype-stained cells and black histograms represent cells positively stained with KDR, CD31, CD146, CD34 and CD45. The percentage of EPC expressing each marker is presented in each case.

FIGURE S3

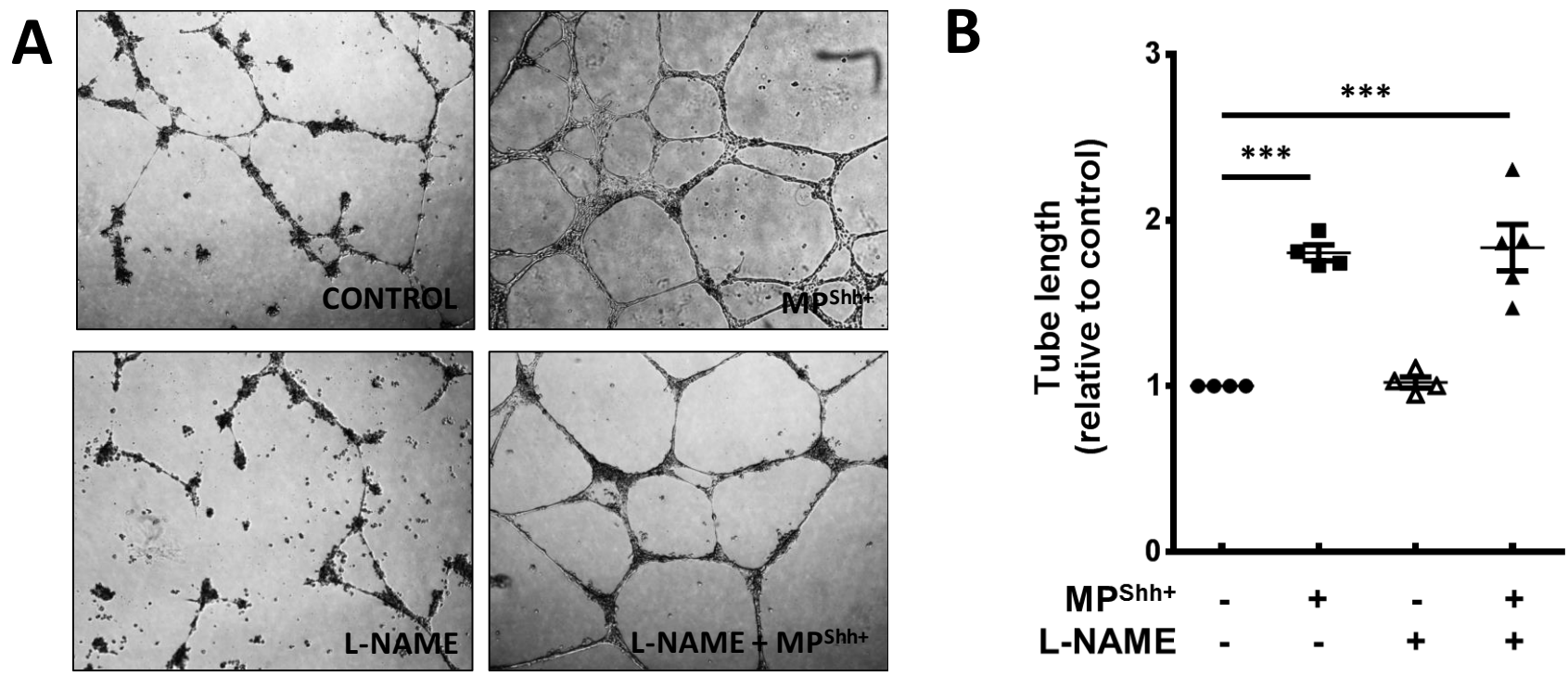


Figure S3. *In vitro* EPC vasculogenesis and NO production. EPC were incubated in the presence or in the absence of 10 $\mu\text{g/mL}$ MP^{Shh+}, pre-incubated or not with 100 μM L-NAME for 24 hours on Matrigel matrix. **(A)** Representative phase-contrast images of capillary-like structures. **(B)** Quantification of total length capillary-like structures expressed relative to control as mean \pm SEM ($n = 4-5$, independent experiments, performed in different cell cultures). *** $p < 0.001$.